Supplementary Information (SI) for Journal of Materials Chemistry C.
This journal is © The Royal Society of Chemistry 2025

Supporting Information

AIEE Active Dual-State Emissive Tripodal Pyridopyrazine Derivatives as Multi-Stimuli Responsive Smart Organic Materials

Monika Lamoria,[a] Debashree Manna,[b] Marilyn Daisy Milton[a*]

[a]*Functional Organic Molecules Synthesis Laboratory, Department of Chemistry, University of Delhi, Delhi-110007, India*

[b]*Institute of Organic Chemistry and Biochemistry, Czech Academy of Sciences, v.v.i., Flemingovo n´am. 2, Prague 6, Praha 16610, Czech Republic*

*Email: mdmilton@chemistry.du.ac.in

1. ^{1}H NMR and ^{13}C NMR spectra of **PP1-PP5**…….....**Fig. S1-S10**
2. HRMS spectra of **PP1-PP5**……..……...…….....**Fig. S11-S15**
3. Crystal data of **PP4**……..……..……..……**Table S1**
4. Emission data in different solvents……...**Table S2**
5. Photophysical properties……**Fig. S16-S27**
6. Average particle size of aggregates……....**Table S3**
7. Limits of detection for **PP1-PP5**…….……..**Table S4**
8. DFT studies…….**Fig. S28-S35**
9. TDDFT absorption and emission wavelengths…….……..**Table S5**
10. Temperature dependent changes for **PP1-PP5**…….……..**Fig. S36**
11. TGA curves for **PP1-PP5**…….……...……...**Fig. S37**

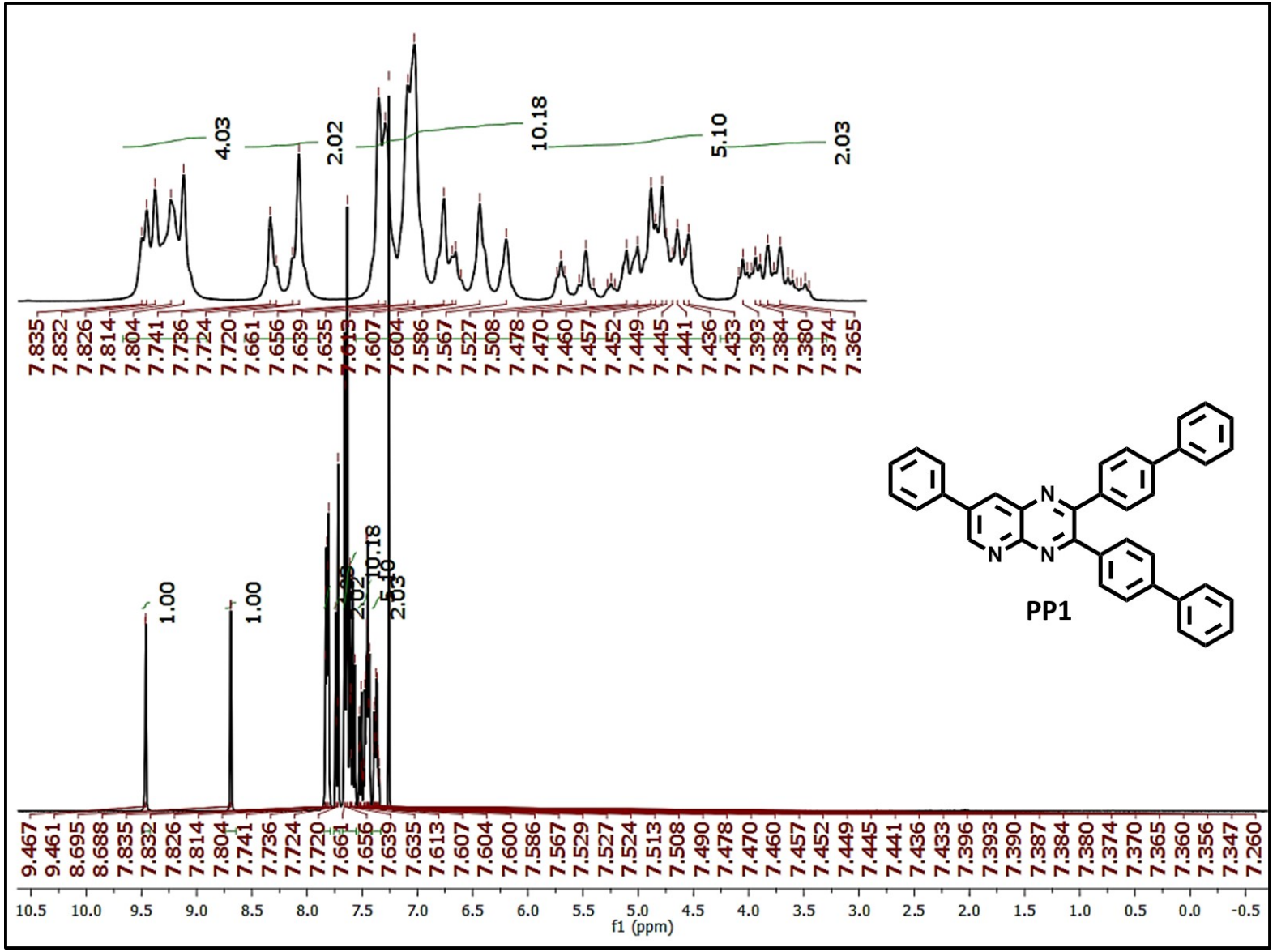

Fig. S1. ^{1}H NMR (400 MHz, $CDCl_3$) spectrum of 2,3-di([1,1'-biphenyl]-4-yl)-7-phenylpyrido[2,3-b]pyrazine (PP1)

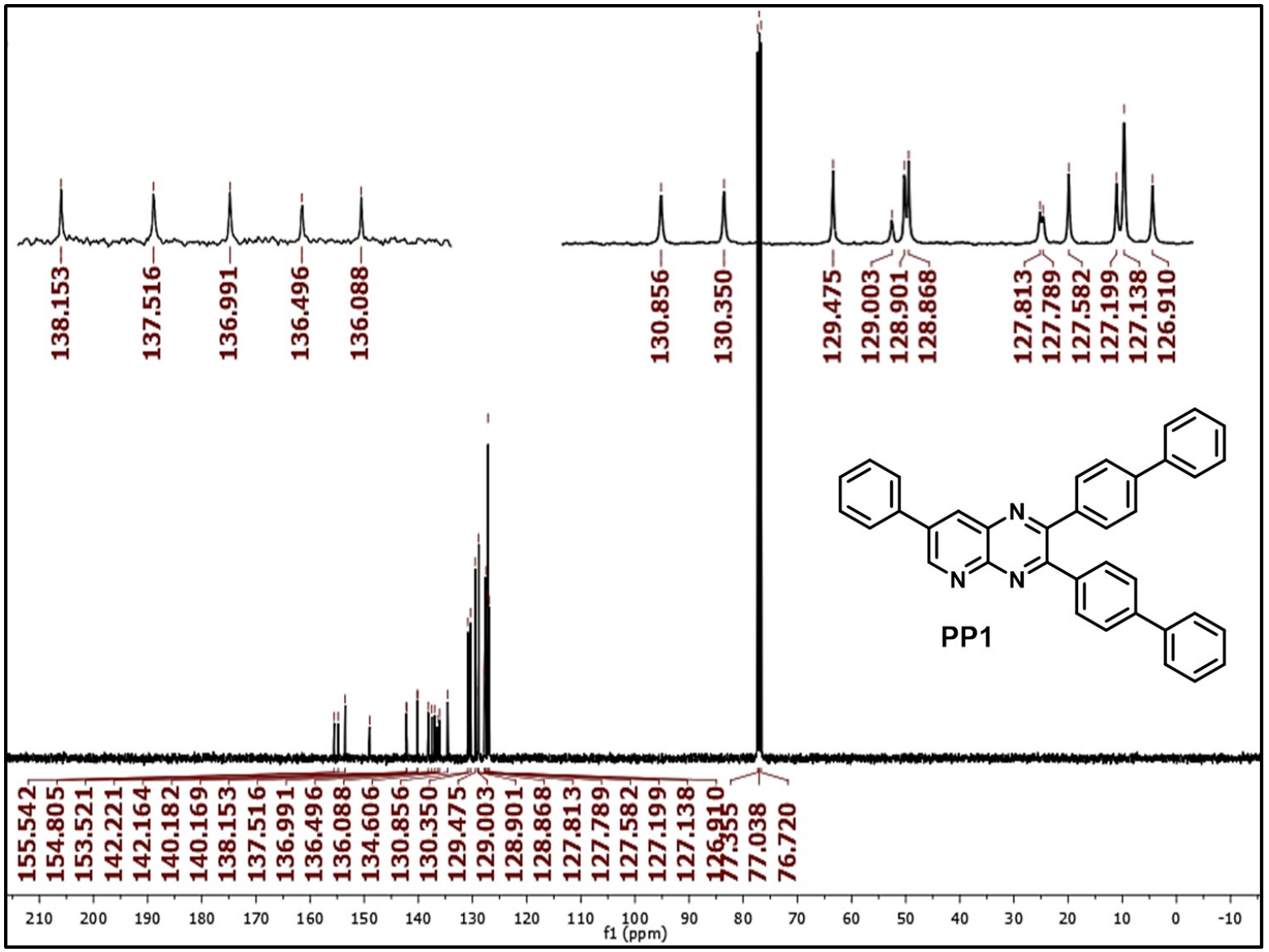

Fig. S2. ^{13}C NMR (100 MHz, $CDCl_3$) spectrum of 2,3-di([1,1'-biphenyl]-4-yl)-7-phenylpyrido[2,3-b]pyrazine (PP1)

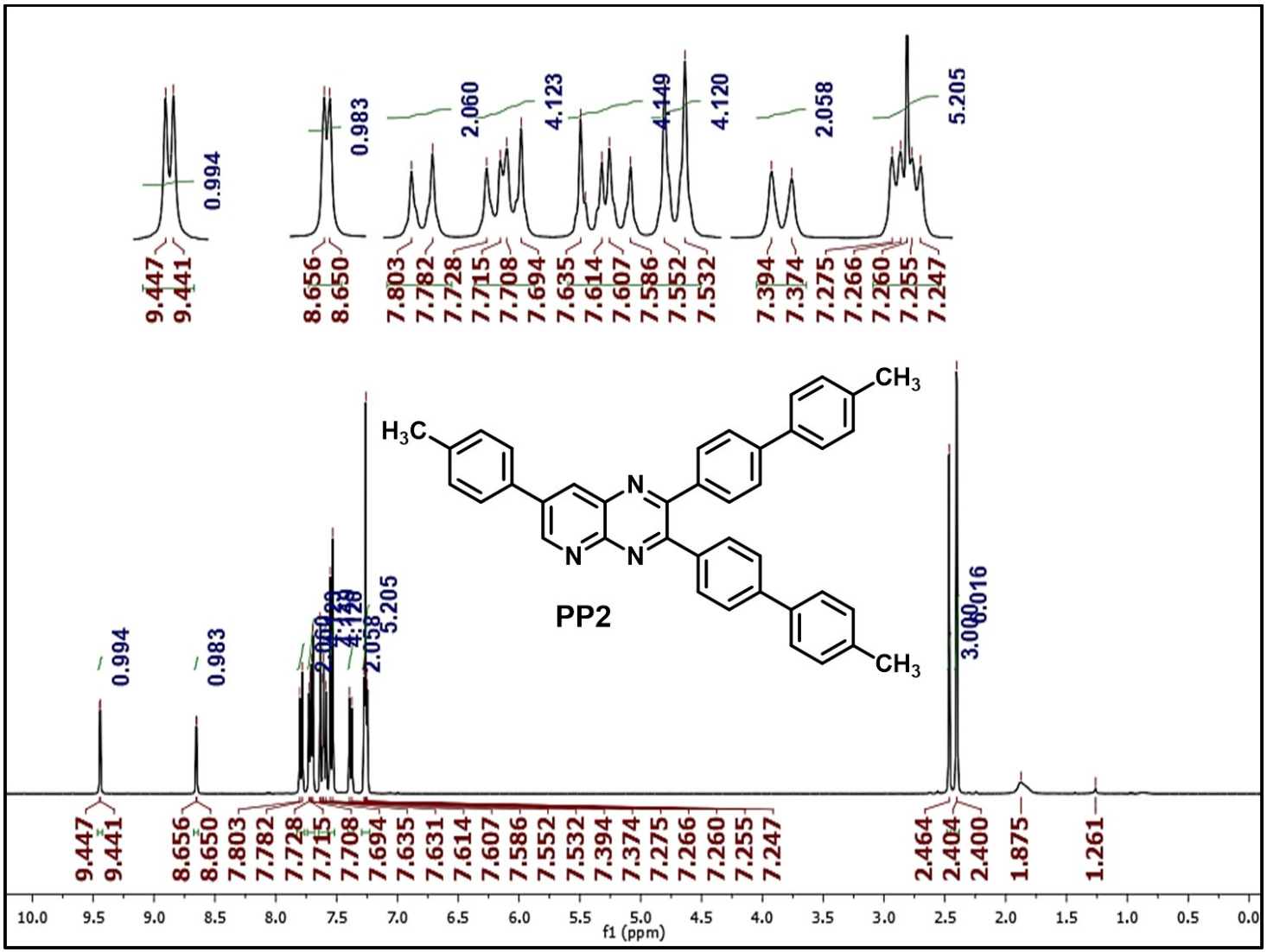

Fig. S3. ^{1}H NMR (400 MHz, $CDCl_3$) spectrum of 2,3-bis(4'-methyl-[1,1'-biphenyl]-4-yl)-7-(p-tolyl)pyrido[2,3-b]pyrazine (PP2)

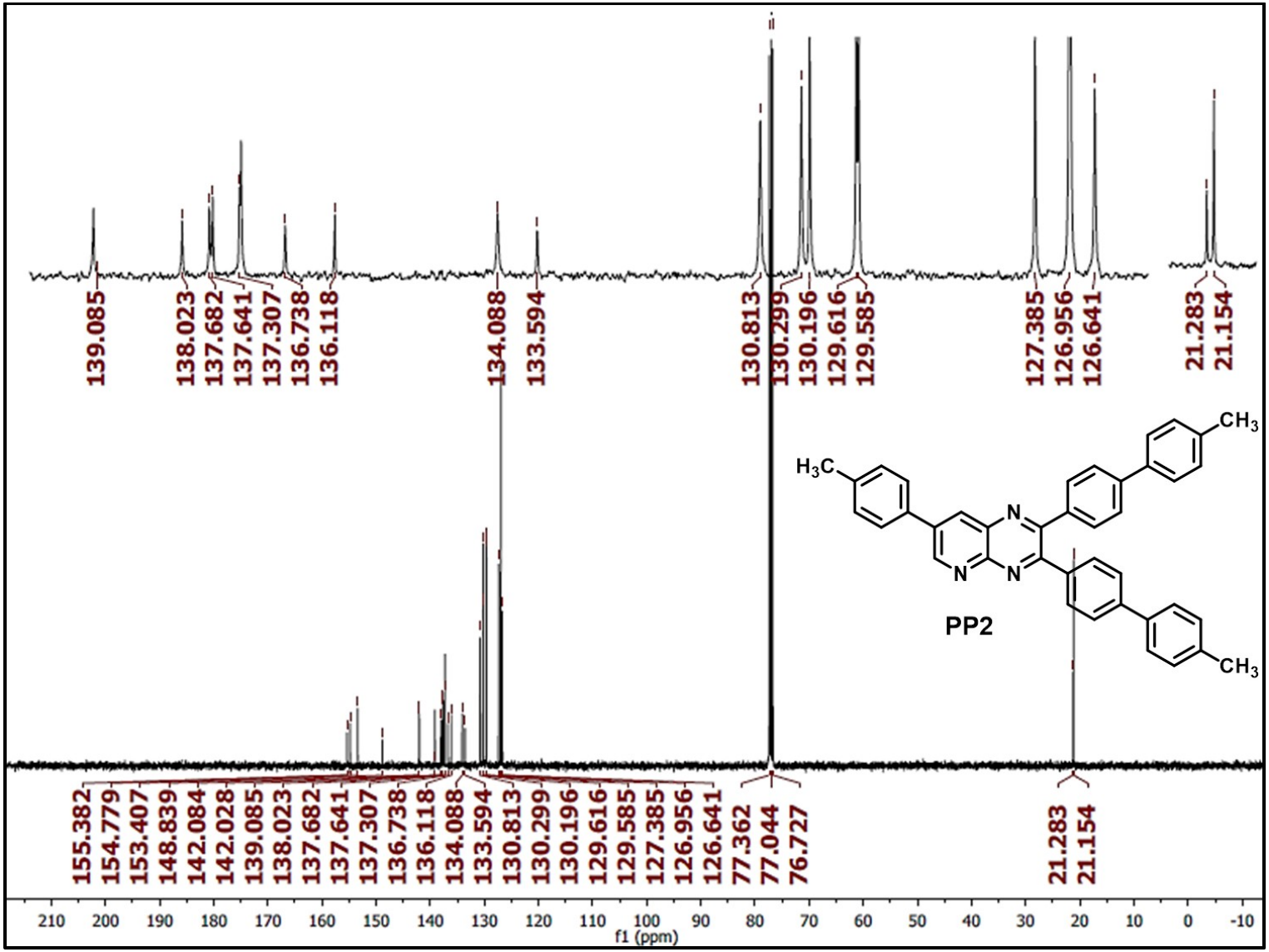

Fig. S4. ^{13}C NMR (100 MHz, $CDCl_3$) spectrum of 2,3-bis(4'-methyl-[1,1'-biphenyl]-4-yl)-7-(p-tolyl)pyrido[2,3-b]pyrazine (PP2)

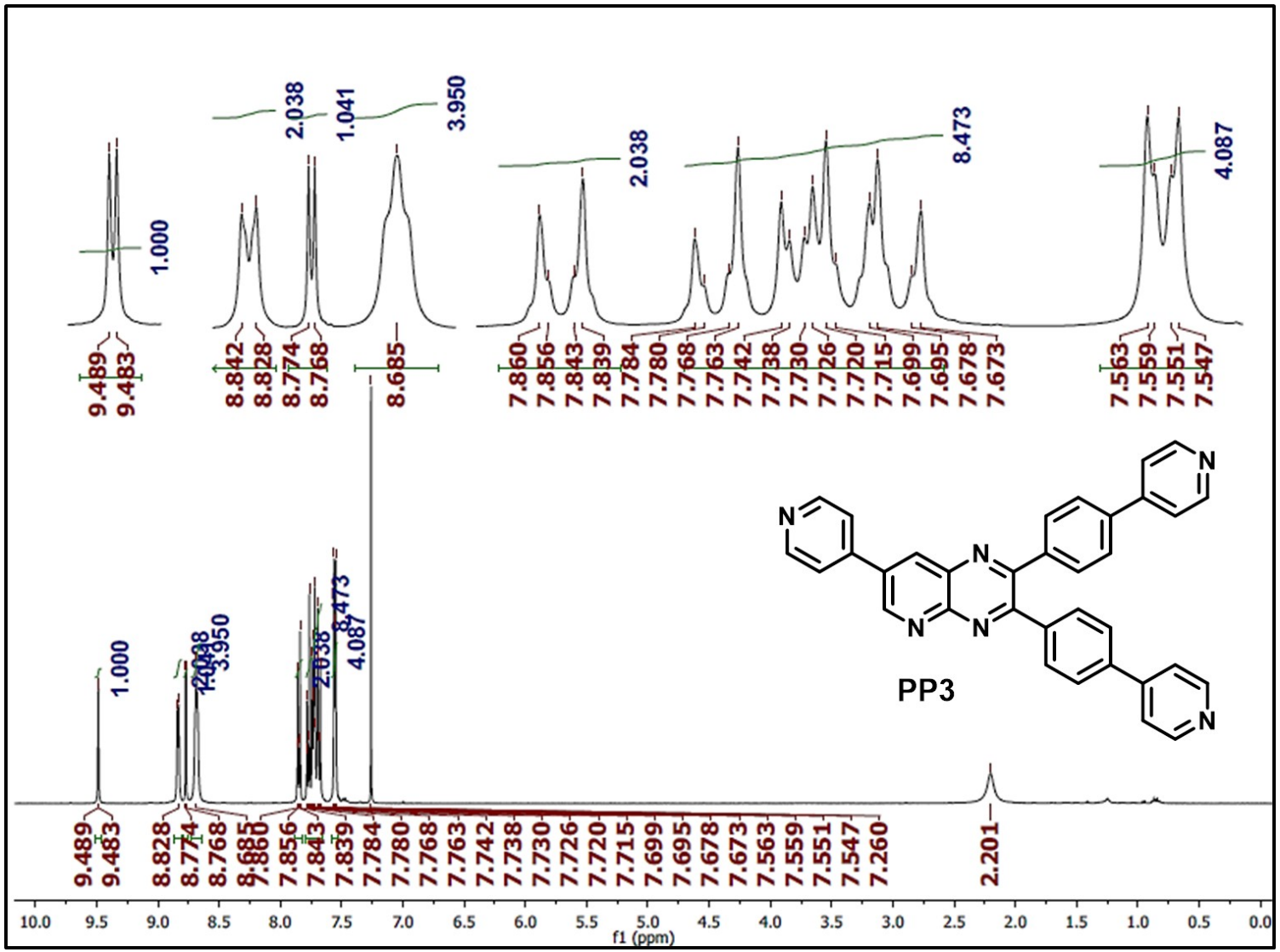

Fig. S5. ^{1}H NMR (400 MHz, $CDCl_3$) spectrum of 7-(pyridin-4-yl)-2,3-bis(4-(pyridin-4-yl)phenyl)pyrido[2,3-b]pyrazine (PP3)

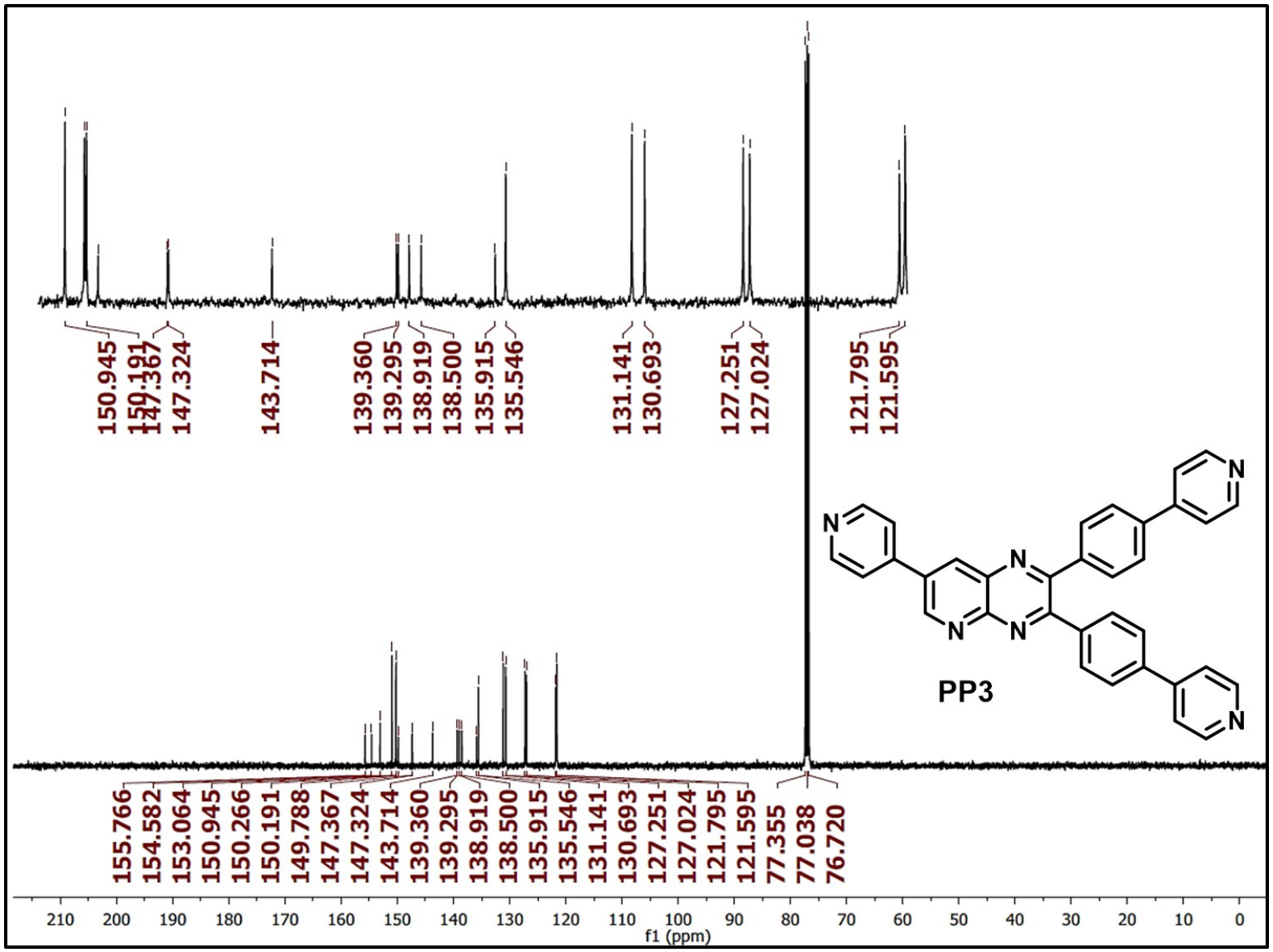

Fig. S6. ^{13}C NMR (100 MHz, $CDCl_3$) spectrum of 7-(pyridin-4-yl)-2,3-bis(4-(pyridin-4-yl)phenyl)pyrido[2,3-b]pyrazine (PP3)

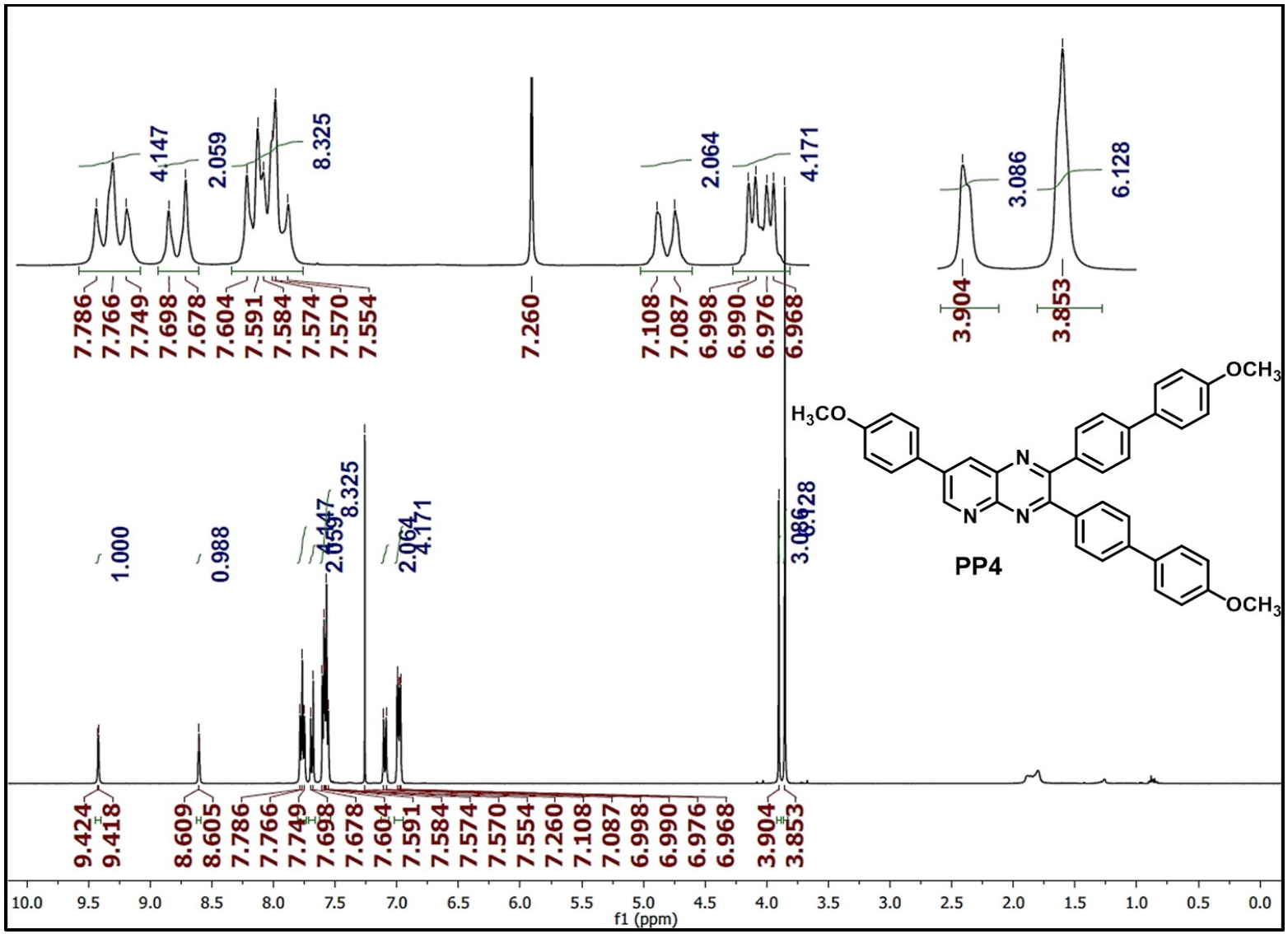

Fig. S7. ^{1}H NMR (400 MHz, $CDCl_3$) spectrum of 2,3-bis(4'-methoxy-[1,1'-biphenyl]-4-yl)-7-(4-methoxyphenyl)pyrido[2,3-b]pyrazine (PP4)

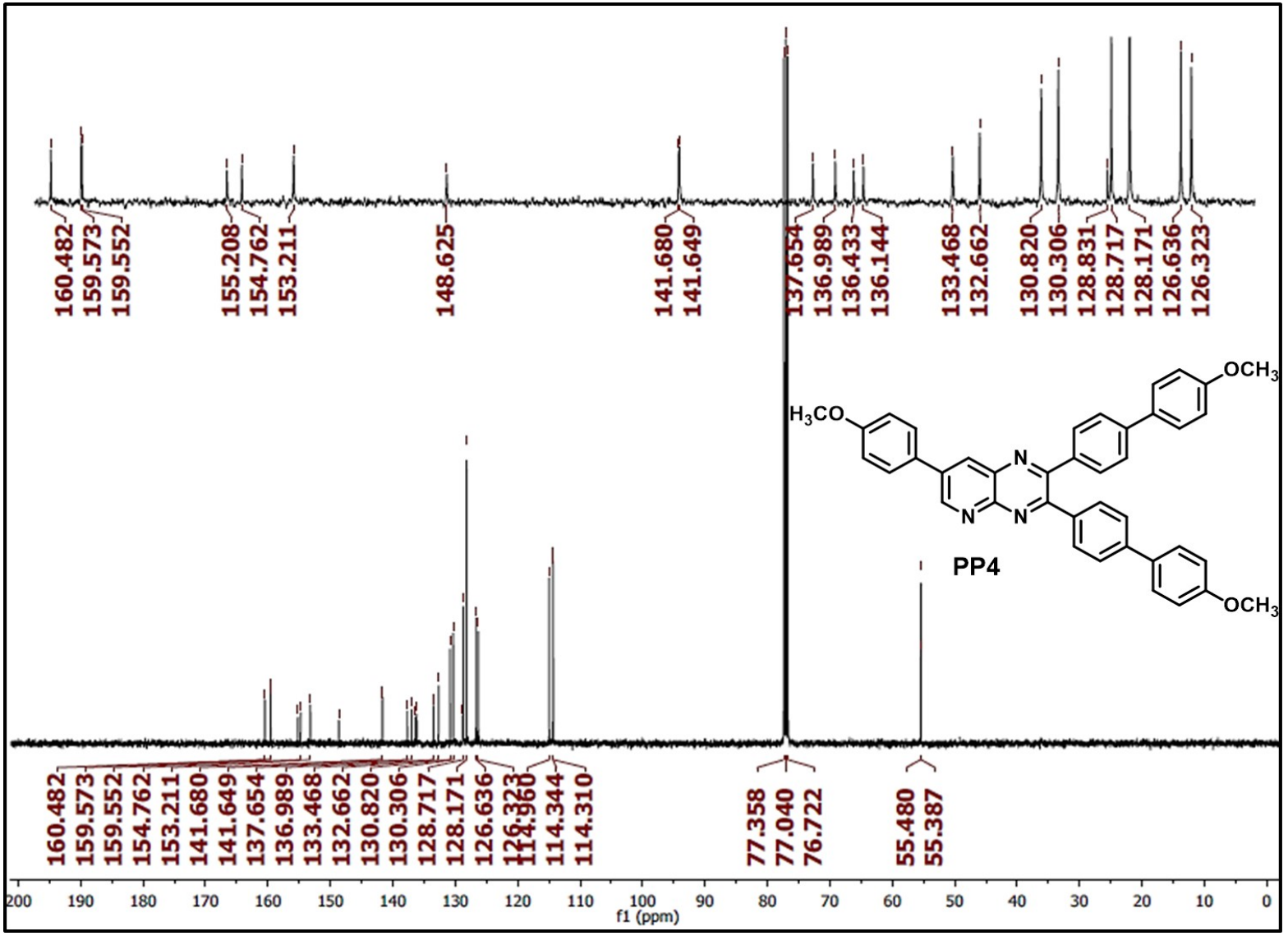

Fig. S8. ^{13}C NMR (100 MHz, $CDCl_3$) spectrum of 2,3-bis(4'-methoxy-[1,1'-biphenyl]-4-yl)-7-(4-methoxyphenyl)pyrido[2,3-b]pyrazine (PP4)

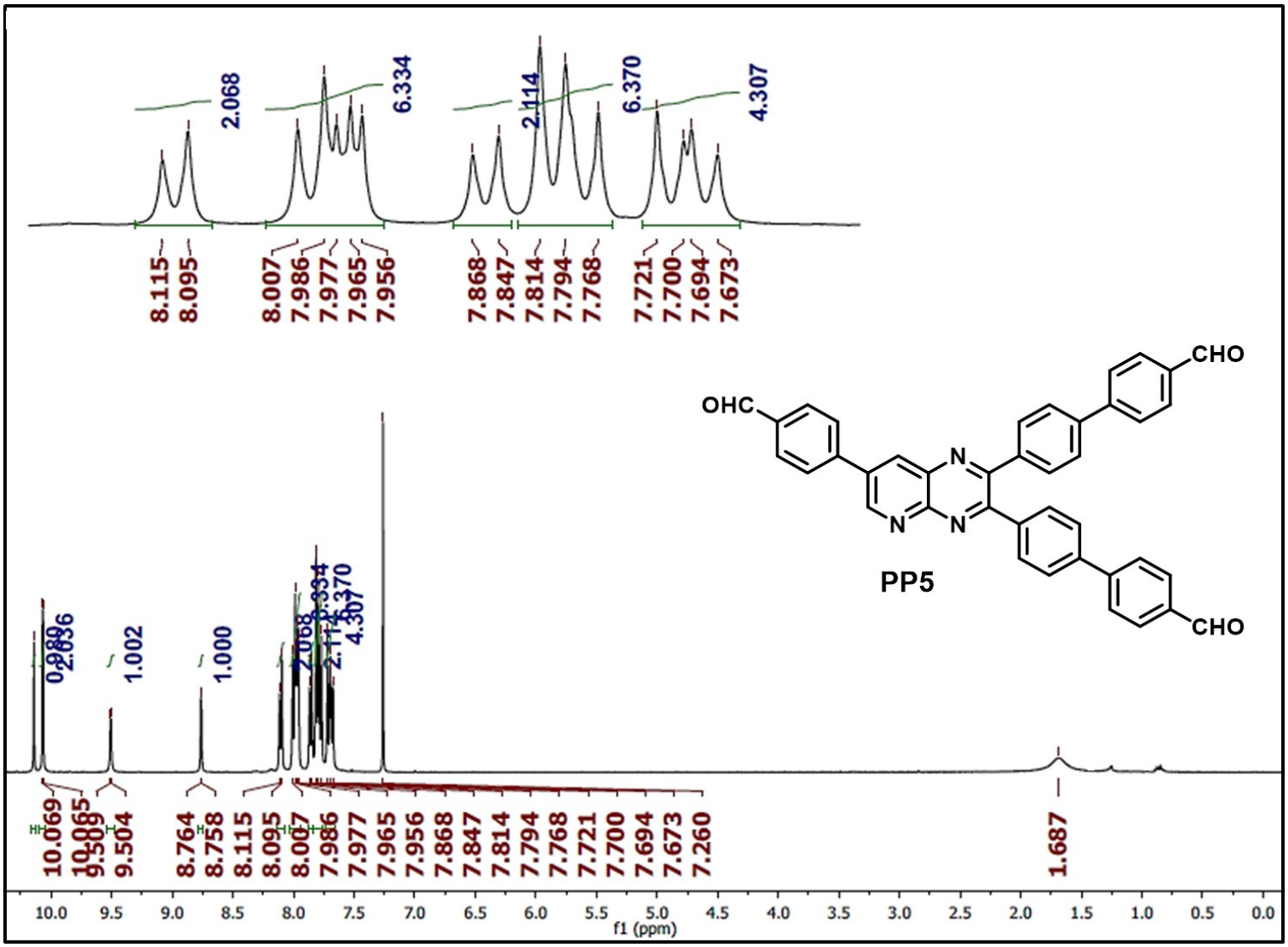

Fig. S9. ^{1}H NMR (400 MHz, $CDCl_3$) spectrum of 4',4'''-(7-(4-formylphenyl)pyrido[2,3-b]pyrazine-2,3-diyl)bis(([1,1'-biphenyl]-4-carbaldehyde)) (PP5)

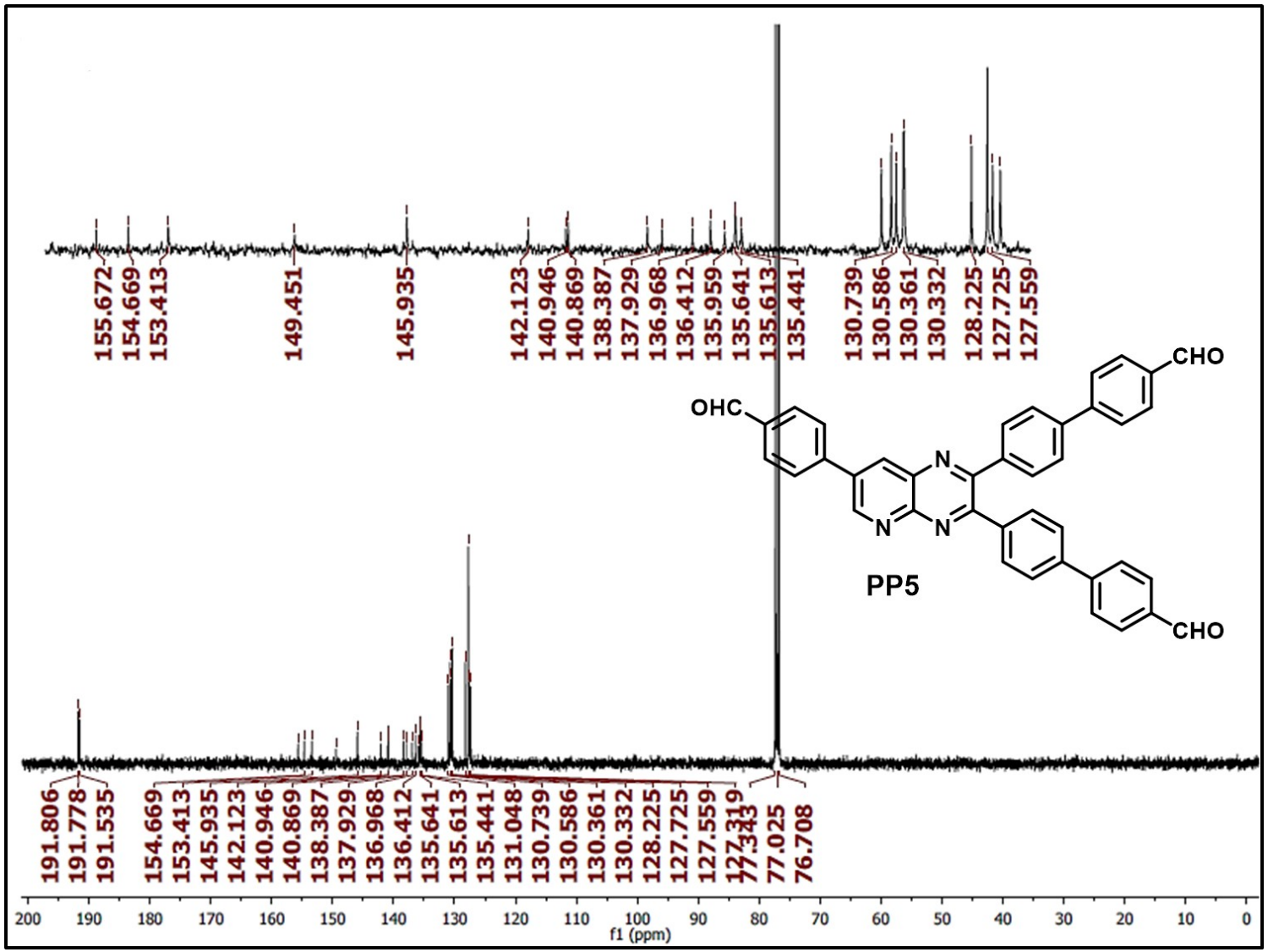

Fig. S10. ^{13}C NMR (100 MHz, $CDCl_3$) spectrum of 4',4'''-(7-(4-formylphenyl)pyrido[2,3-b]pyrazine-2,3-diyl)bis(([1,1'-biphenyl]-4-carbaldehyde)) (PP5)

Compound Table

Compound Label	RT	Mass	Abund	Formula	Tgt Mass	Diff (ppm)	MFG Formula	DB Formula
Cpd 1: C37 H25 N3	0.078	511.2057	737667	C37 H25 N3	511.2048	1.58	C37 H25 N3	C37 H25 N3

Compound Label	*m/z*	RT	Algorithm	Mass
Cpd 1: C37 H25 N3	512.213	0.078	Find By Formula	511.2057

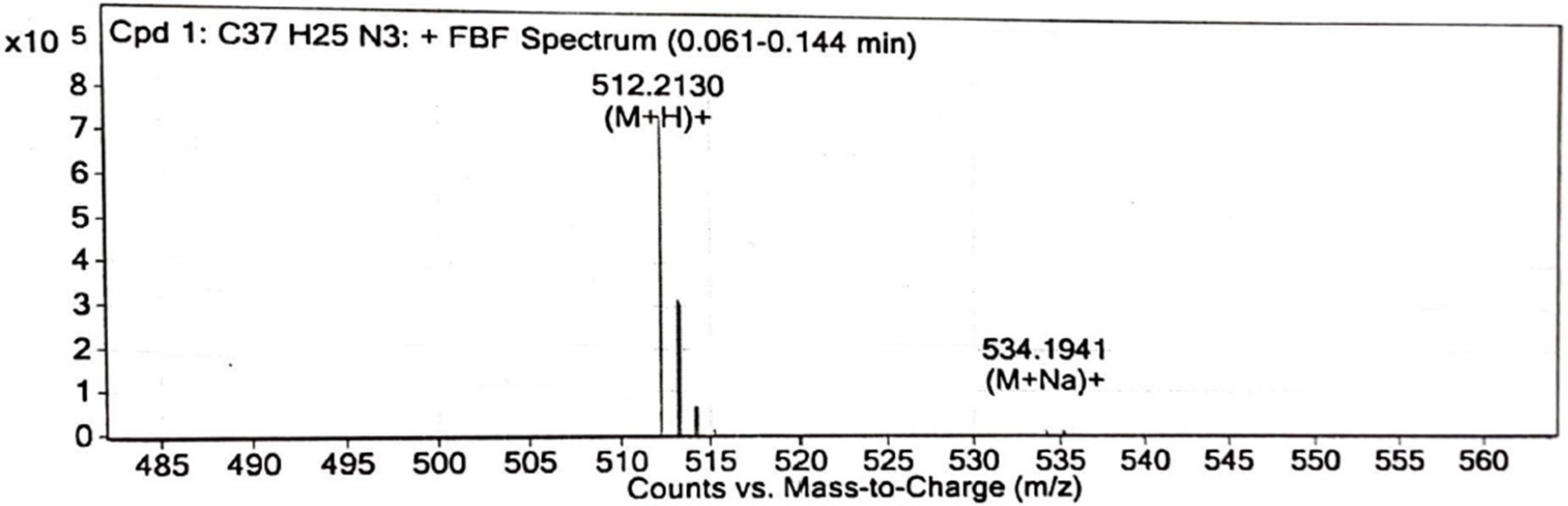

Fig. S11. HRMS spectrum of 2,3-di([1,1'-biphenyl]-4-yl)-7-phenylpyrido[2,3-b]pyrazine (PP1)

Compound Table

Compound Label	RT	Mass	Abund	Formula	Tgt Mass	Diff (ppm)	MFG Formula	DB Formula
Cpd 1: C40 H31 N3	0.089	553.2522	312621	C40 H31 N3	553.2518	0.72	C40 H31 N3	C40 H31 N3

Compound Label	*m/z*	RT	Algorithm	Mass
Cpd 1: C40 H31 N3	554.2596	0.089	Find By Formula	553.2522

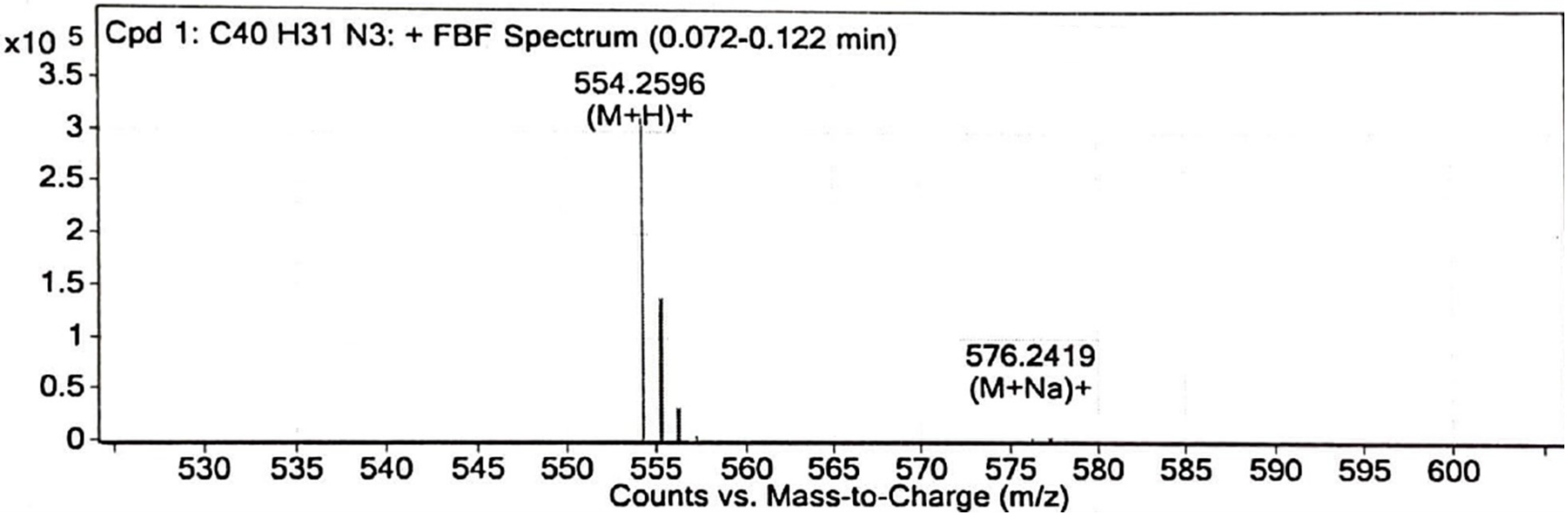

Fig. S12. HRMS spectrum of 2,3-bis(4'-methyl-[1,1'-biphenyl]-4-yl)-7-(p-tolyl)pyrido[2,3-b]pyrazine (PP2)

Compound Table

Compound Label	RT	Mass	Abund	Formula	Tgt Mass	Diff (ppm)	MFG Formula	DB Formula
Cpd 1: C34 H22 N6	0.103	514.1911	387435	C34 H22 N6	514.1906	1.05	C34 H22 N6	C34 H22 N6

Compound Label	*m/z*	RT	Algorithm	Mass
Cpd 1: C34 H22 N6	515.1988	0.103	Find By Formula	514.1911

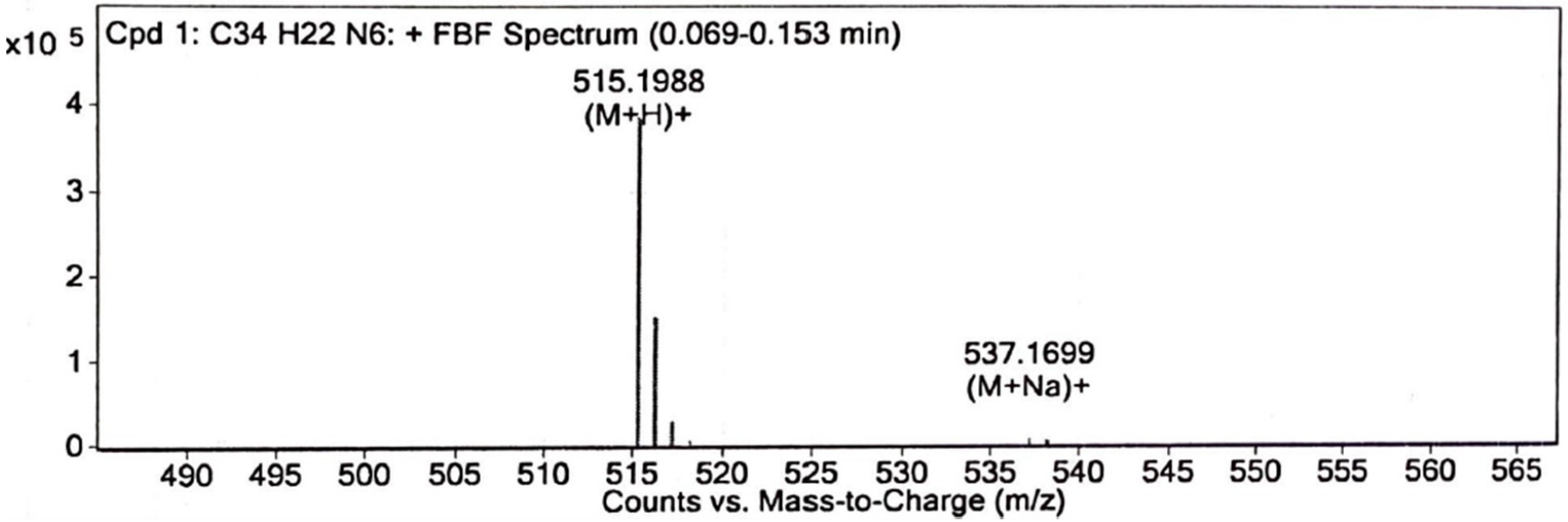

Fig. S13. HRMS spectrum of 7-(pyridin-4-yl)-2,3-bis(4-(pyridin-4-yl)phenyl)pyrido[2,3-b]pyrazine (PP3)

Compound Table

Compound Label	RT	Mass	Abund	Formula	Tgt Mass	Diff (ppm)	MFG Formula	DB Formula
Cpd 1: C40 H31 N3 O3	0.086	601.237	358117	C40 H31 N3 O3	601.2365	0.73	C40 H31 N3 O3	C40 H31 N3 O3

Compound Label	*m/z*	RT	Algorithm	Mass
Cpd 1: C40 H31 N3 O3	602.2443	0.086	Find By Formula	601.237

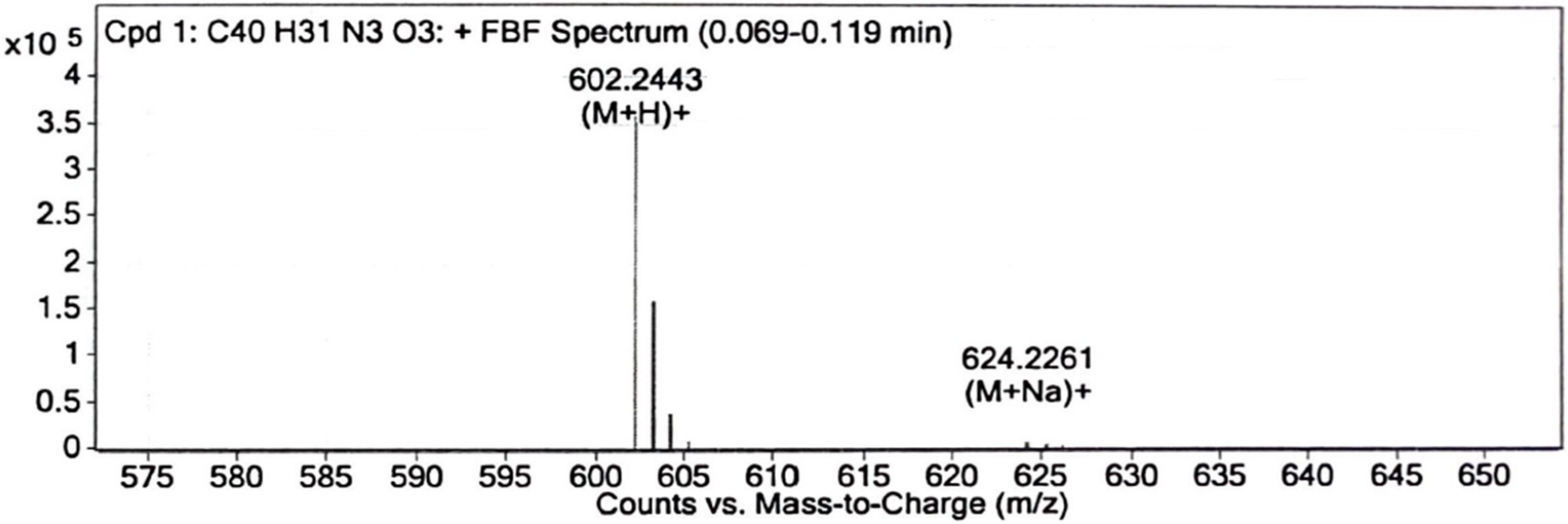

Fig. S14. HRMS spectrum of 2,3-bis(4'-methoxy-[1,1'-biphenyl]-4-yl)-7-(4-methoxyphenyl)pyrido[2,3-b]pyrazine (PP4)

Compound Table

Compound Label	RT	Mass	Abund	Formula	Tgt Mass	Diff (ppm)	MFG Formula	DB Formula
Cpd 1: C40 H25 N3 O3	0.083	595.1893	130738	C40 H25 N3 O3	595.1896	-0.51	C40 H25 N3 O3	C40 H25 N3 O3

Compound Label	*m/z*	RT	Algorithm	Mass
Cpd 1: C40 H25 N3 O3	596.1967	0.083	Find By Formula	595.1893

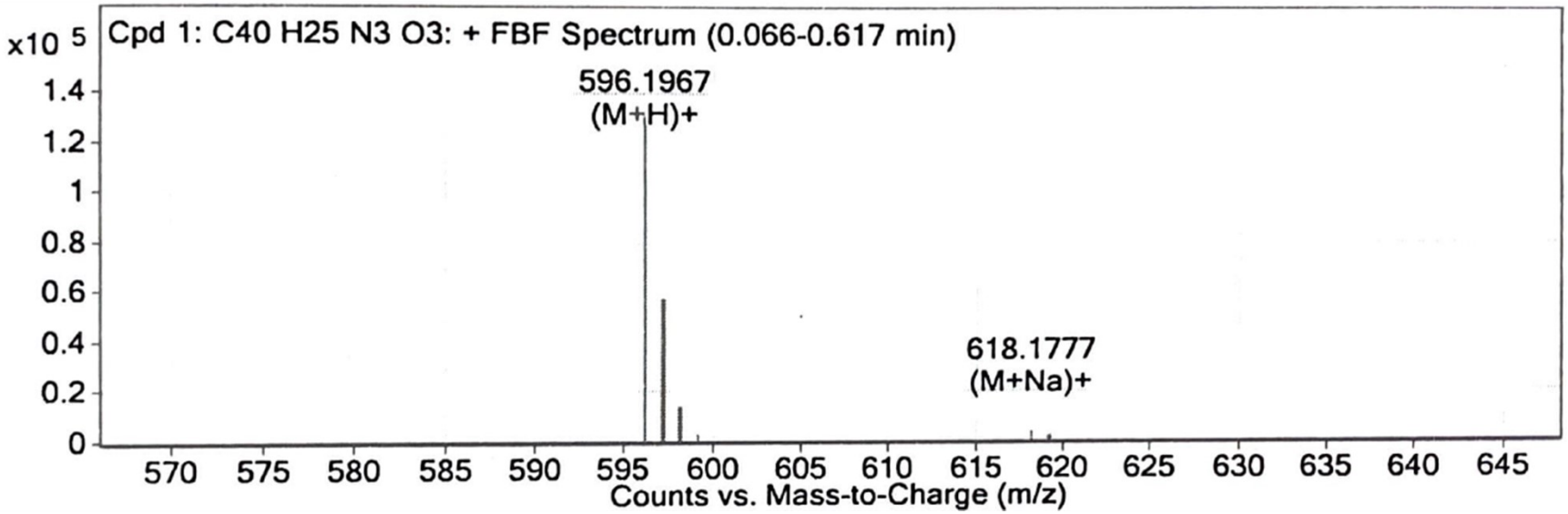

Fig. S15. HRMS spectrum of 4',4'''-(7-(4-formylphenyl)pyrido[2,3-b]pyrazine-2,3-diyl)bis(([1,1'-biphenyl]-4-carbaldehyde)) (PP5)

Table S1. Crystal data and structure refinement for PP4

Identification code	PP4
Empirical formula	$C_{40}H_{31}N_3O_3$
Formula weight	601.710
Temperature/K	298.0
Crystal system	Monoclinic
Space group	P21/c
a/Å	13.2222(5)
b/Å	21.5979(8)
c/Å	12.2263(4)
α/°	90
β/°	116.927(2)
γ/°	90
Volume/Å3	3113.0(2)
Z	4
ρcalcg/cm3	1.284
μ/mm-1	0.649
F(000)	1267.9
Crystal size/mm3	0.335 × 0.206 × 0.031
Radiation	Cu Kα (λ = 1.54178)
2Θ range for data collection/°	7.5 to 137.16
Index ranges	-15 ≤ h ≤ 15, -25 ≤ k ≤ 26, -14 ≤ l ≤ 14
Reflections collected	52329
Independent reflections	5639 [Rint = 0.0863, Rsigma = 0.0539]
Data/restraints/parameters	5639/0/429
Goodness-of-fit on F2	1.118
Final R indexes [I>=2σ (I)]	R1 = 0.0917, wR2 =0.2514
Final R indexes [all data]	R1 = 0.1336, wR2 = 0.3320
Largest diff. peak/hole / e Å-3	0.26/-0.37

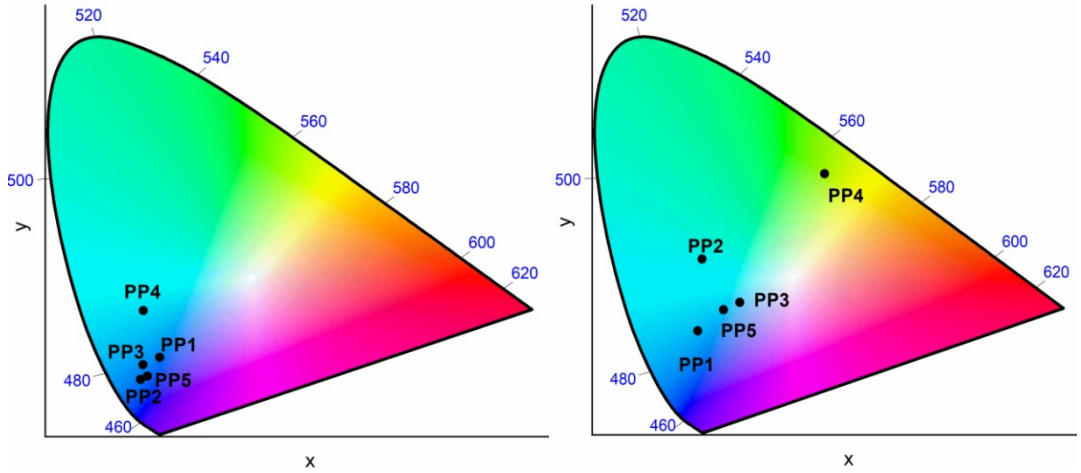

Fig. S16. CIE chromaticity diagrams for **PP1-PP5** in solution and solid state respectively.

Table S2: The emission data of compounds **PP1**, **PP2** and **PP4** in solvents of differing polarity.

	Compound	**Toluene**	**THF**	**$CHCl_3$**	**CH_3CN**	**DMSO**	**$\Delta\lambda_{em}$ (nm)**
λ_{em} (nm)	**PP1**	446	448	447	449	456	10
	PP2	440	449	455	456	467	18
	PP4	455	473	475	499	518	63

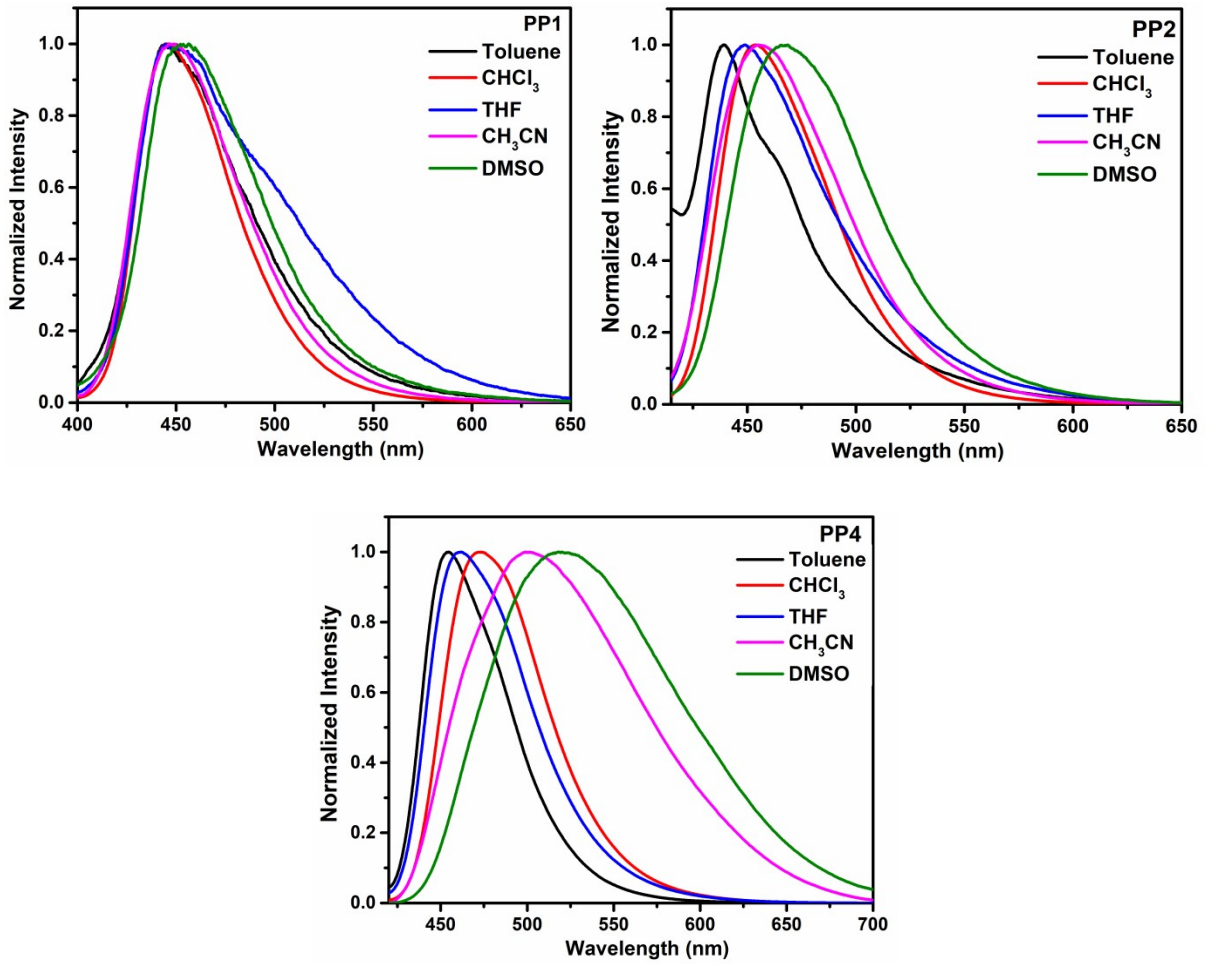

Fig. S17. Normalized emission spectra of **PP1-PP2** and **PP4** (2×10^{-5} M) in solvents of differing polarity.

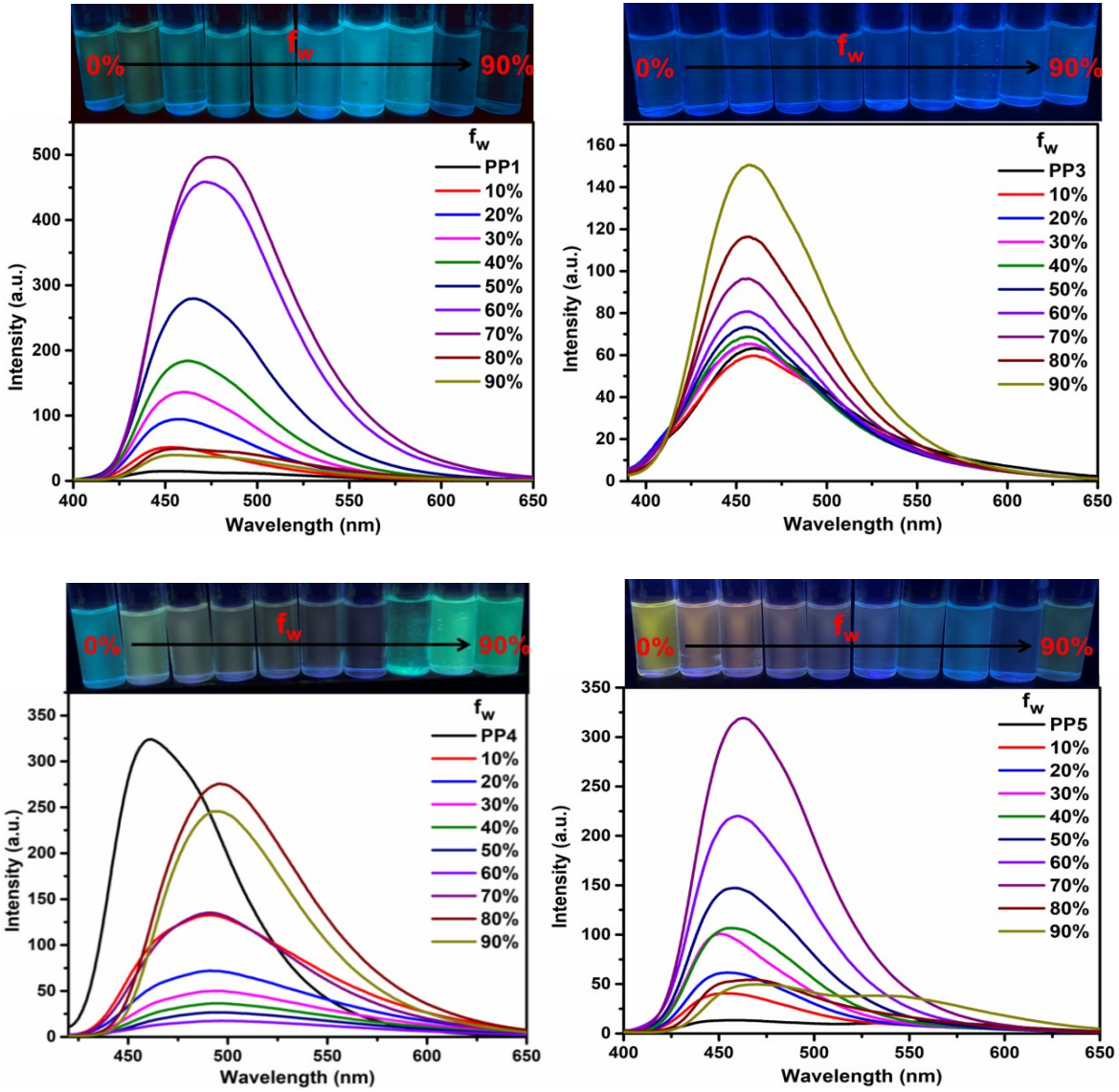

Fig. S18. Emission spectra of **PP1, PP3-PP5** (2×10^{-5}M) in THF-H_2O fractions.

Table S3: Average particle size of the aggregates at different THF-H_2O fractions.

Compound	f_w (%H_2O)	Average diameter (nm)
PP1	0	420.6
	70	1800
	90	715.6
PP2	0	761.3
	50	1575
	90	803.8
PP3	0	442.6
	90	3316
PP4	0	1969
	70	3134
	90	2133
PP5	0	924
	80	1957
	90	1279

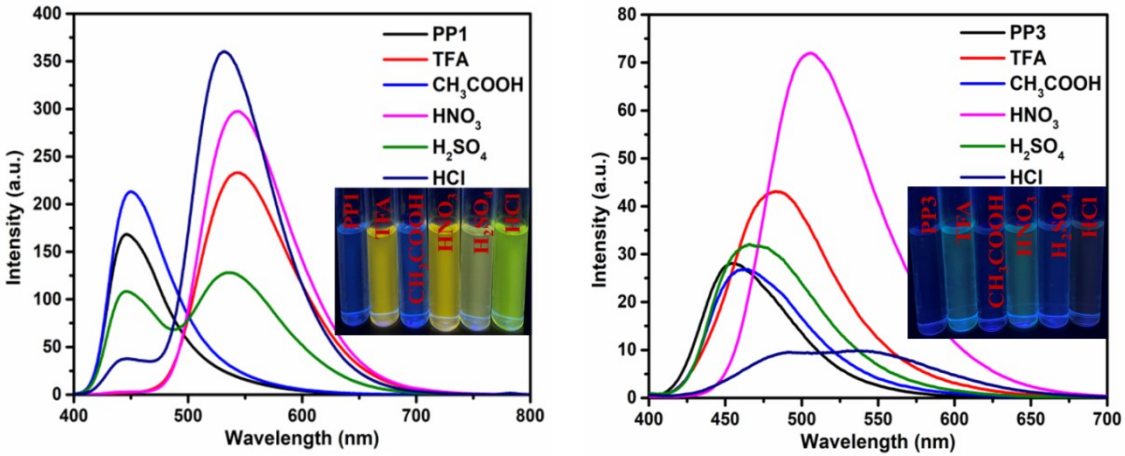

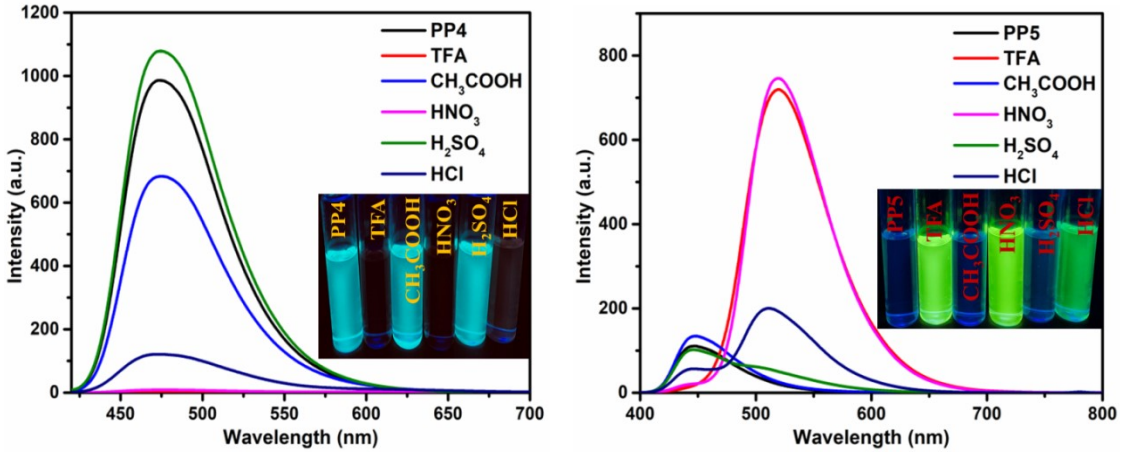

Fig. S19. The emission spectra of **PP1**, **PP3-PP5** (2×10^{-5}M) in presence of 0.02 mL of different acids in $CHCl_3$.

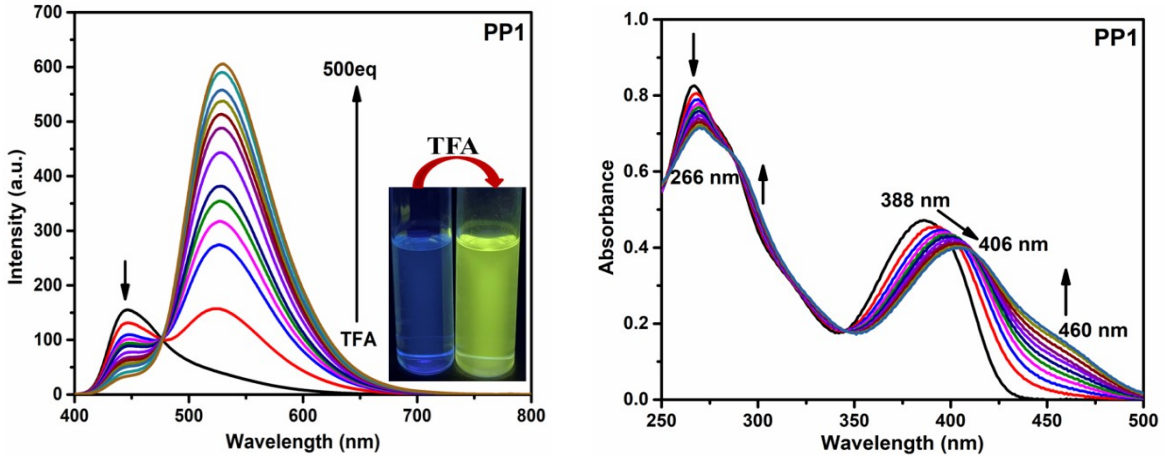

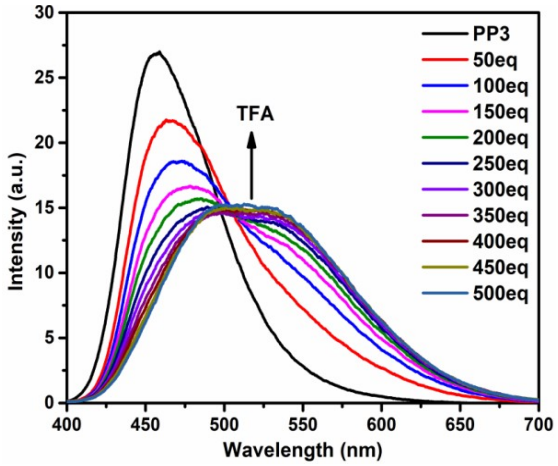
PP3
50eq
100eq
150eq
200eq
250eq
300eq
350eq
400eq
450eq
500eq
TFA
Intensity (a.u.)
Wavelength (nm)

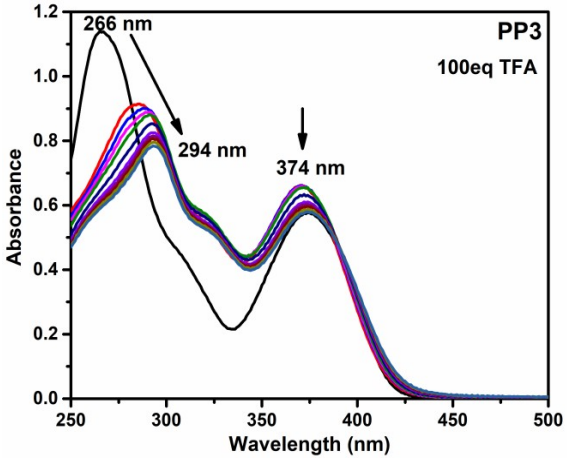
PP3
100eq TFA
266 nm
294 nm
374 nm
Absorbance
Wavelength (nm)

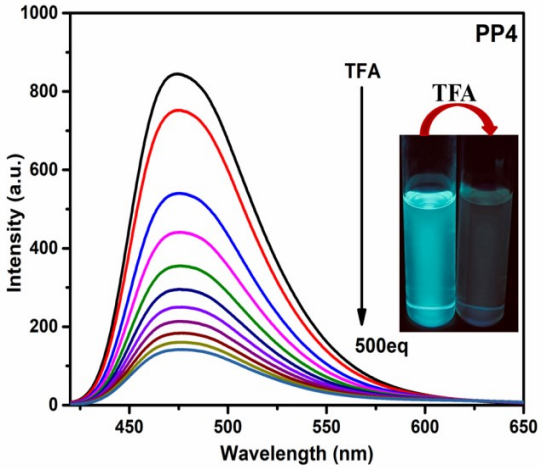
PP4
TFA
TFA
500eq
Intensity (a.u.)
Wavelength (nm)

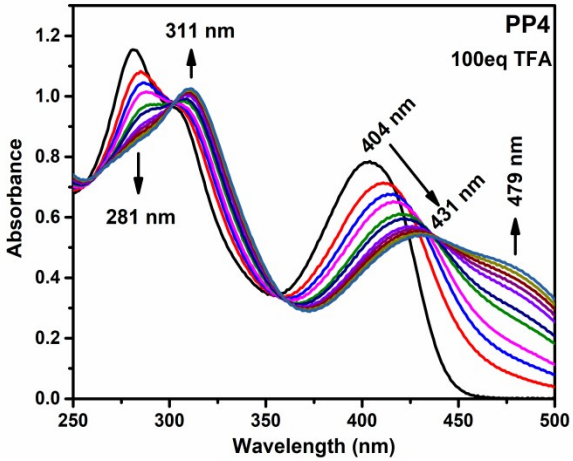
PP4
100eq TFA
311 nm
281 nm
404 nm
431 nm
479 nm
Absorbance
Wavelength (nm)

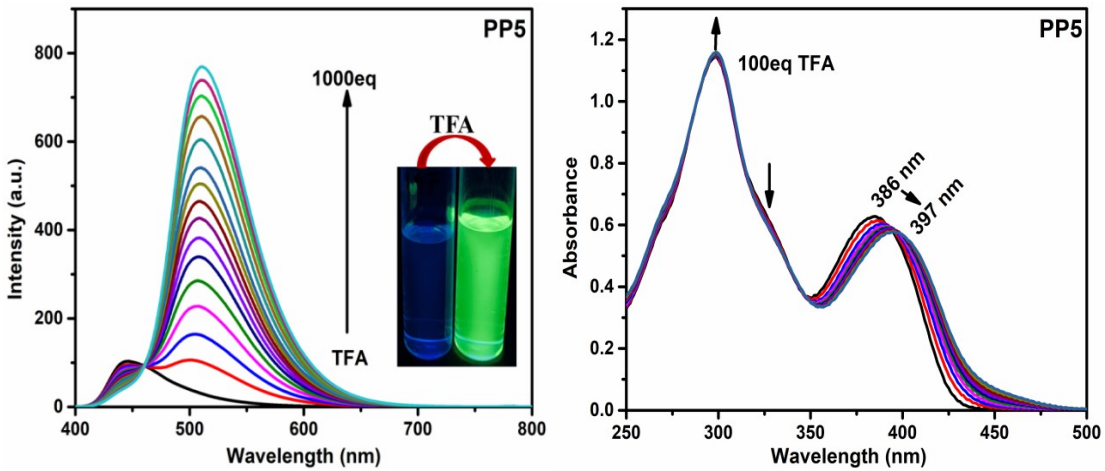

Fig. S20. The emission (2×10^{-5} M) and absorption (1×10^{-5} M) spectra of **PP1**, **PP3-PP5** as a function of the concentration of TFA added in $CHCl_3$. Inset: Photographs in $CHCl_3$ before and after addition of TFA under UV light (365 nm).

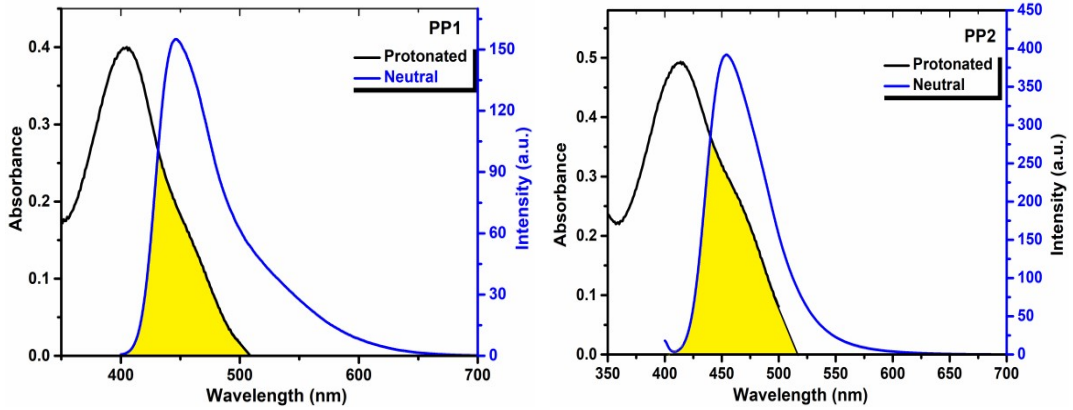

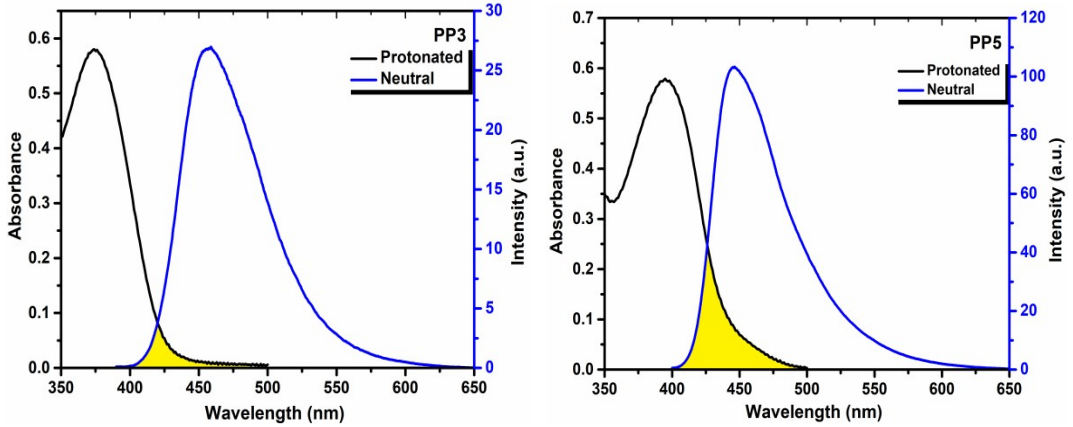

Fig. S21. Spectral overlap between the absorbance of protonated form and emission of neutral form of **PP1**, **PP3** and **PP5** in $CHCl_3$.

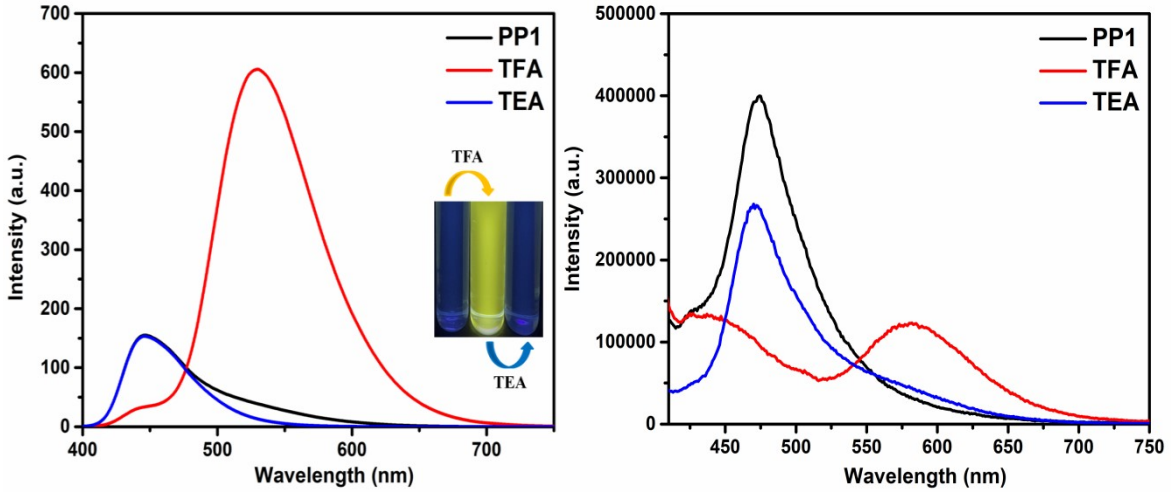

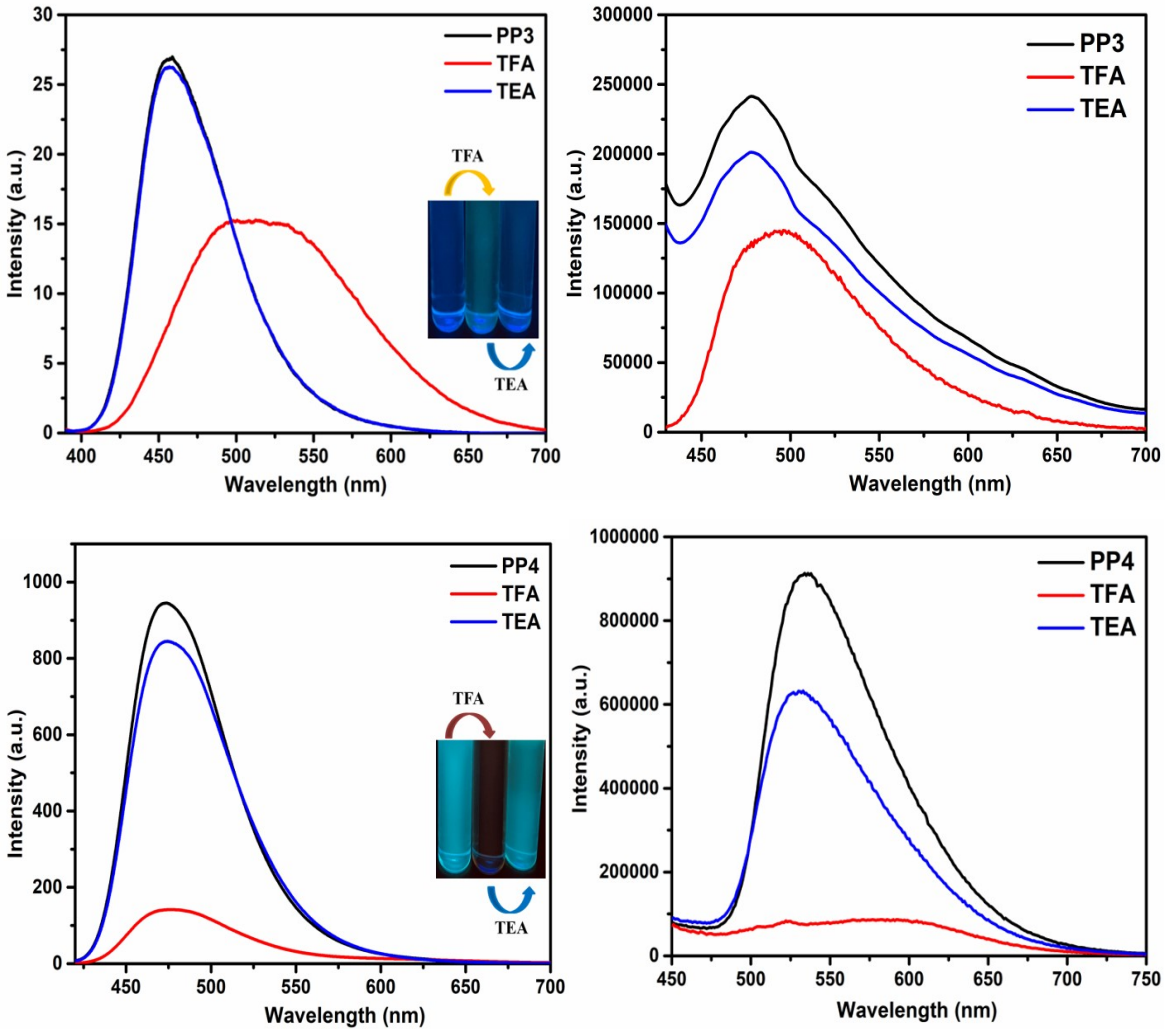
PP3
TFA
TEA
Intensity (a.u.)
Wavelength (nm)
PP4
TFA
TEA
Intensity (a.u.)
Wavelength (nm)

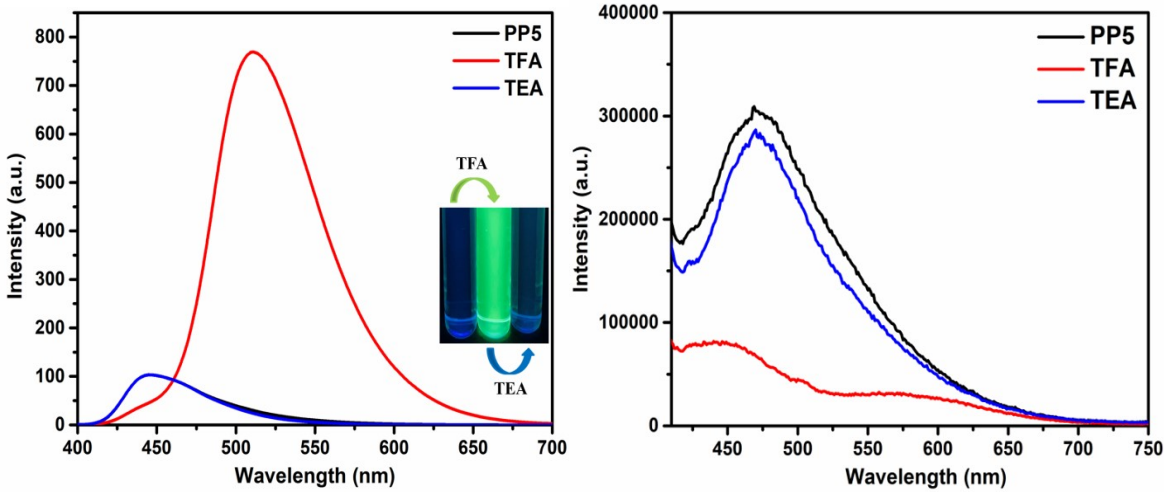

Fig. S22. Emission spectra of **PP1**, **PP3-PP5** after sequential addition of TFA and TEA in $CHCl_3$ (inset: Images after sequential addition of TFA and TEA in $CHCl_3$ under UV light) and solid state.

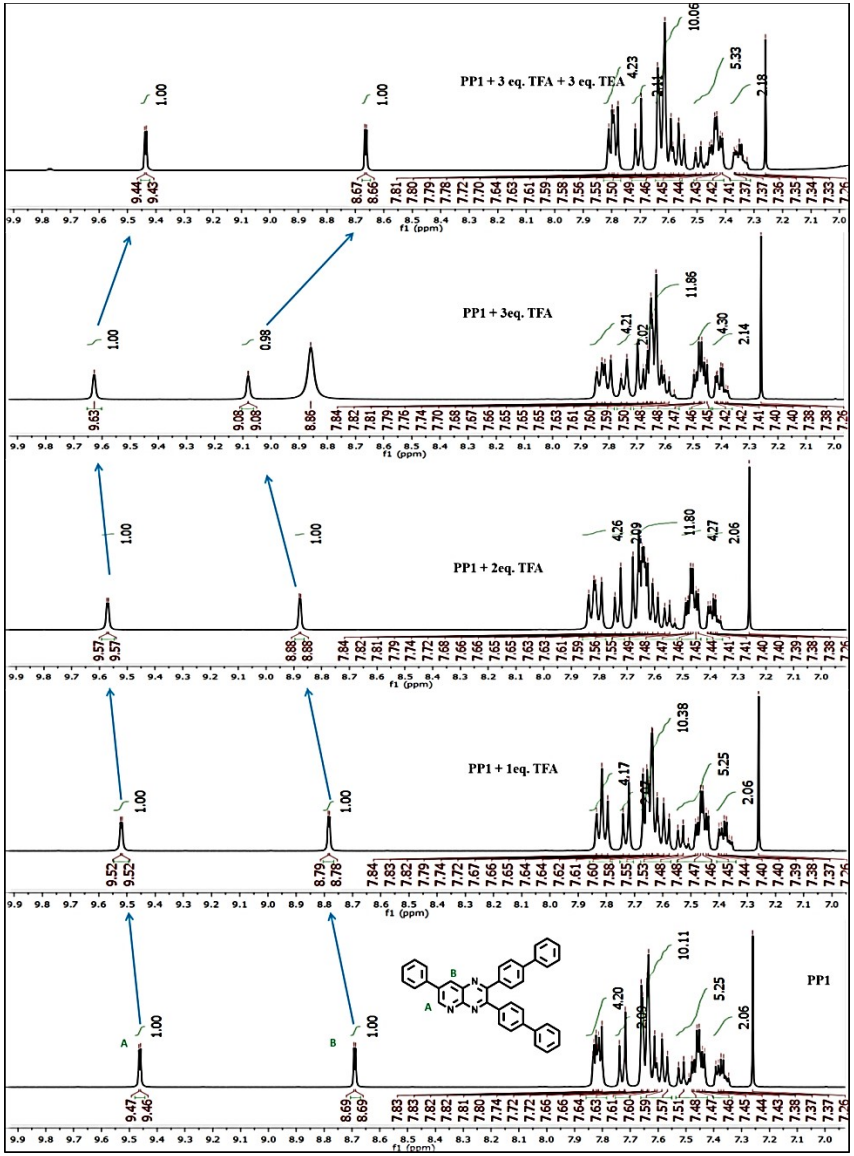

Fig. S23. Partial ^{1}H-NMR (400 MHz, $CDCl_3$) titration spectra of **PP1** on sequential addition of 3 eq. of TFA and TEA.

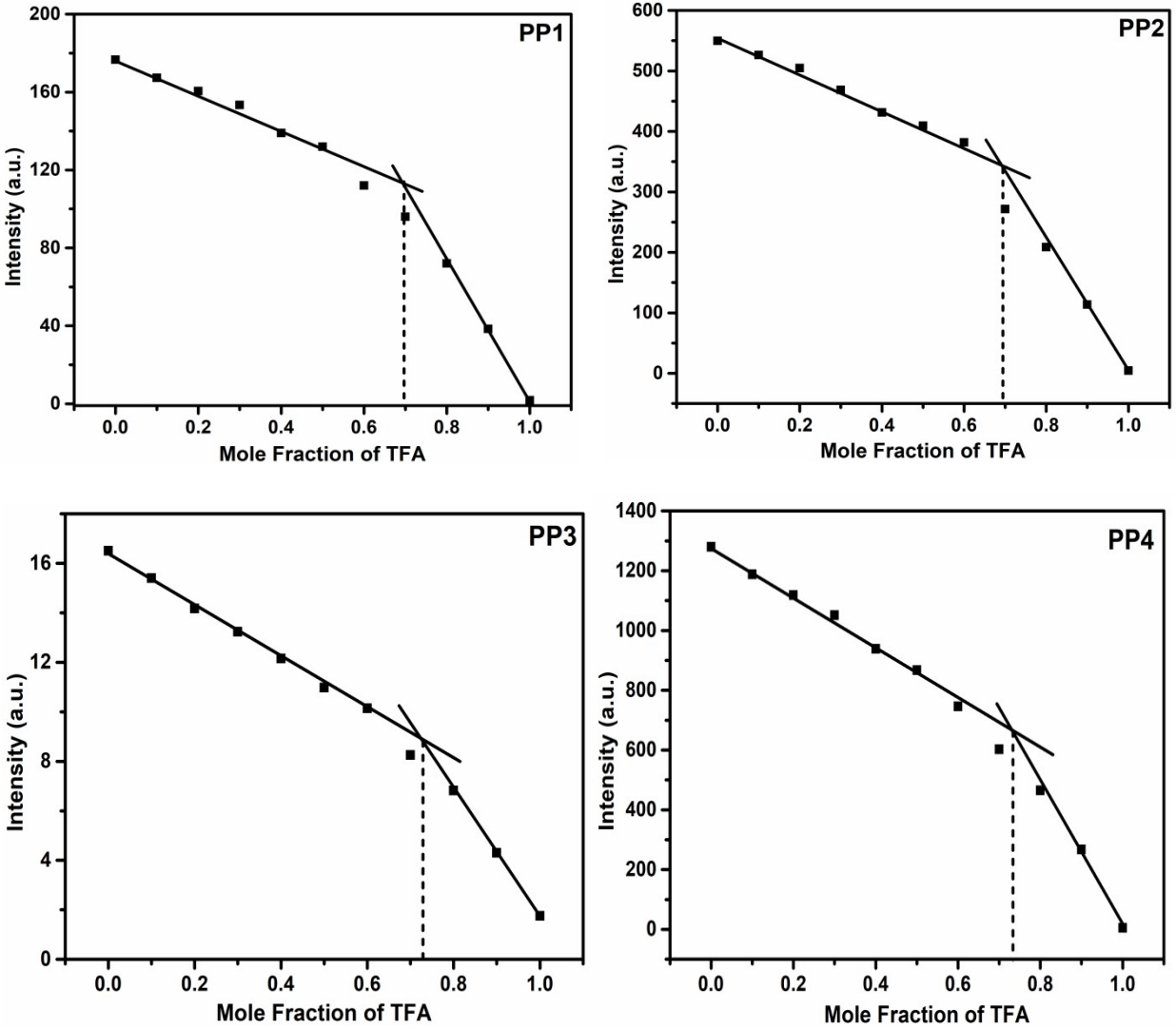
PP1
Intensity (a.u.)
Mole Fraction of TFA
PP2
Intensity (a.u.)
Mole Fraction of TFA
PP3
Intensity (a.u.)
Mole Fraction of TFA
PP4
Intensity (a.u.)
Mole Fraction of TFA

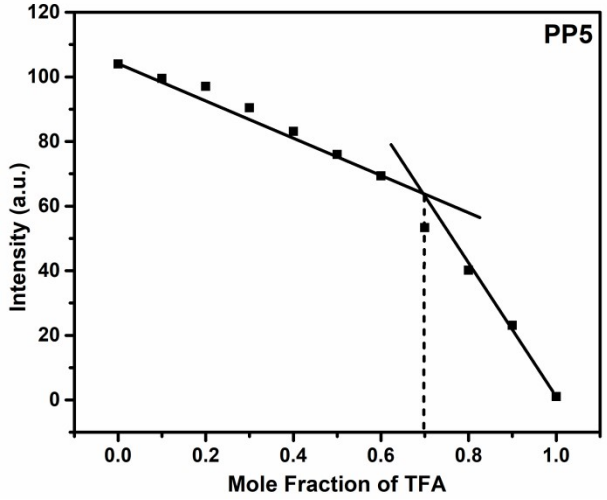

Fig. S24. Jobs plot to find binding stoichiometry of **PP1-PP5** (1×10^{-5} M) with TFA in $CHCl_3$.

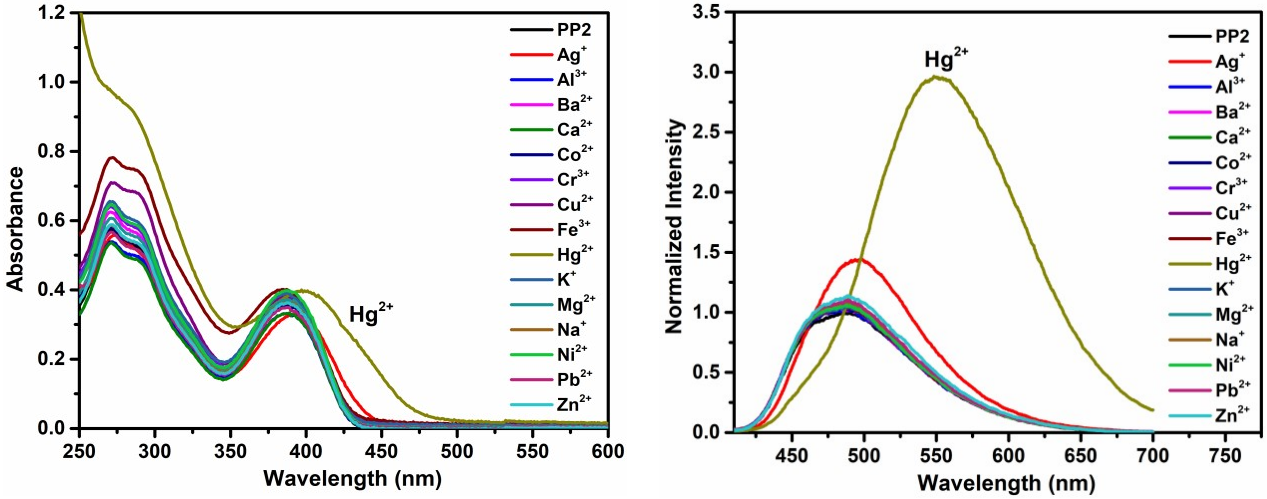

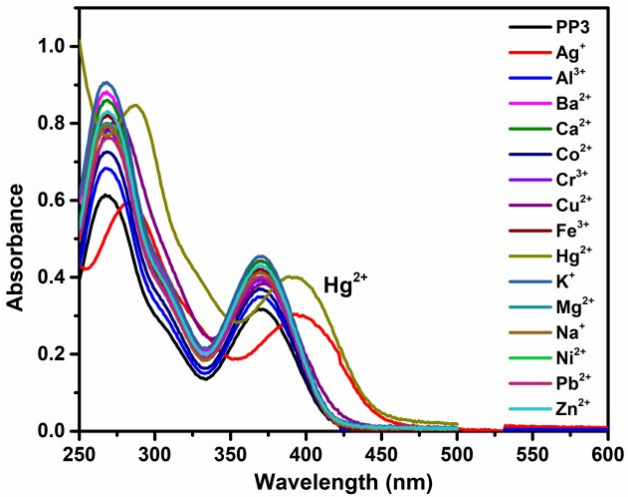
Absorbance
Wavelength (nm)
Hg2+
PP3
Ag+
Al3+
Ba2+
Ca2+
Co2+
Cr3+
Cu2+
Fe3+
Hg2+
K+
Mg2+
Na+
Ni2+
Pb2+
Zn2+

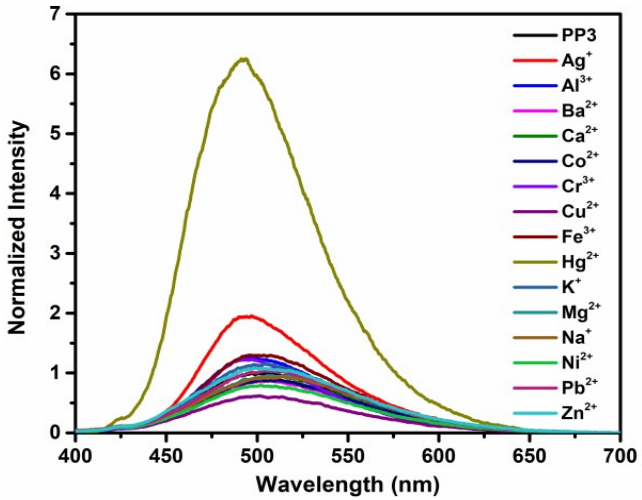
Normalized Intensity
Wavelength (nm)
PP3
Ag+
Al3+
Ba2+
Ca2+
Co2+
Cr3+
Cu2+
Fe3+
Hg2+
K+
Mg2+
Na+
Ni2+
Pb2+
Zn2+

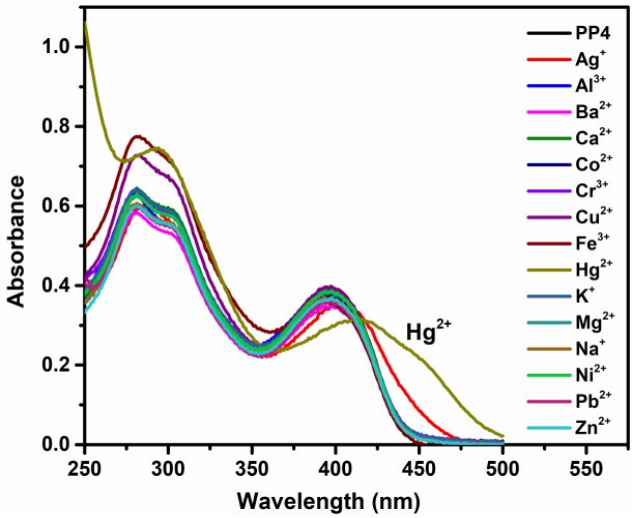
Absorbance
Wavelength (nm)
Hg2+
PP4
Ag+
Al3+
Ba2+
Ca2+
Co2+
Cr3+
Cu2+
Fe3+
Hg2+
K+
Mg2+
Na+
Ni2+
Pb2+
Zn2+

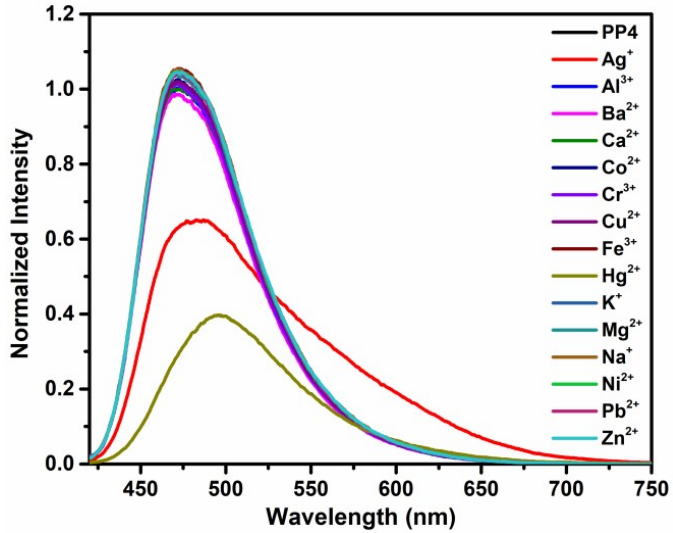
Normalized Intensity
Wavelength (nm)
PP4
Ag+
Al3+
Ba2+
Ca2+
Co2+
Cr3+
Cu2+
Fe3+
Hg2+
K+
Mg2+
Na+
Ni2+
Pb2+
Zn2+

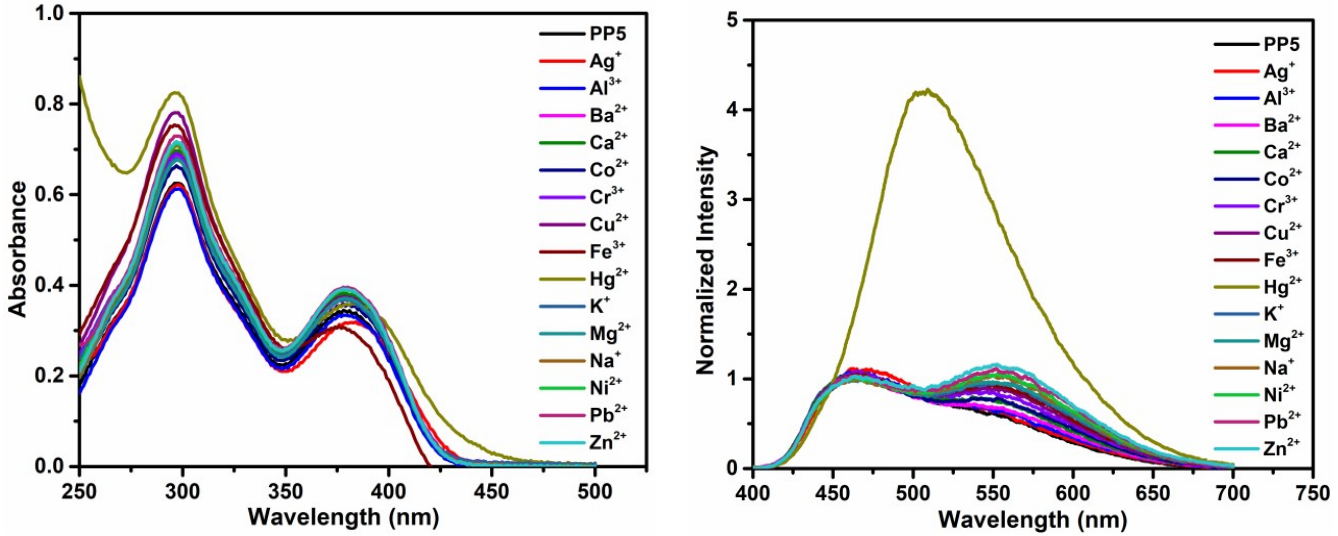

Fig. S25. Absorption and emission spectra of **PP2-PP5** showing selectivity of probes towards Hg^{2+} in presence of other competitive metal ions in THF-H_2O mixtures.

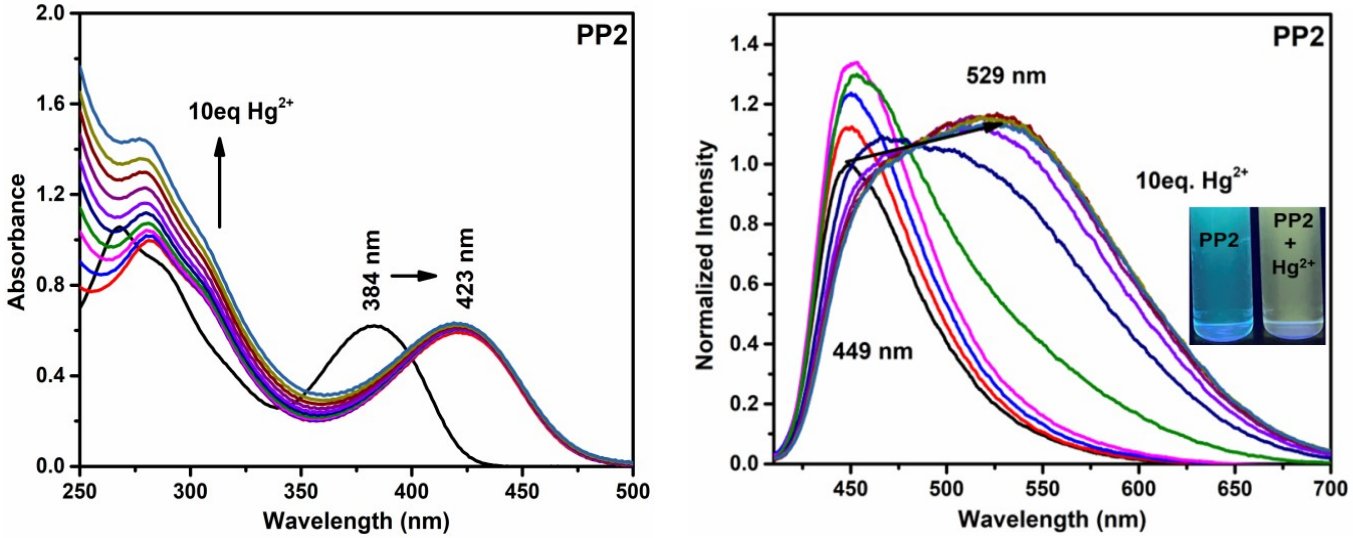

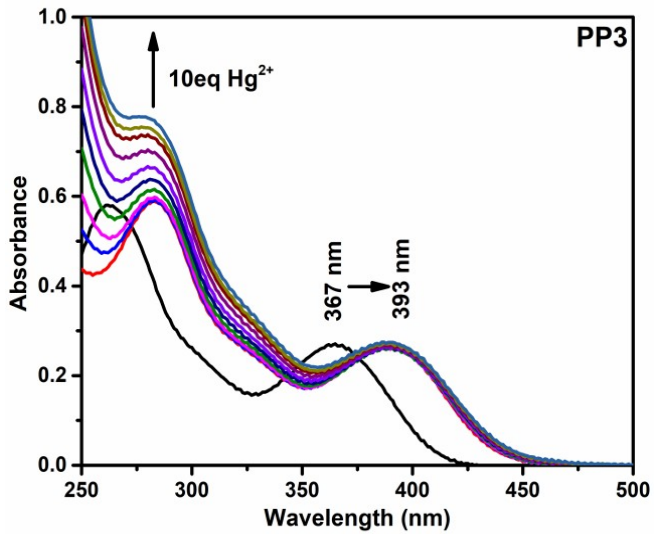
PP3
10eq Hg2+
Absorbance
Wavelength (nm)
367 nm
393 nm

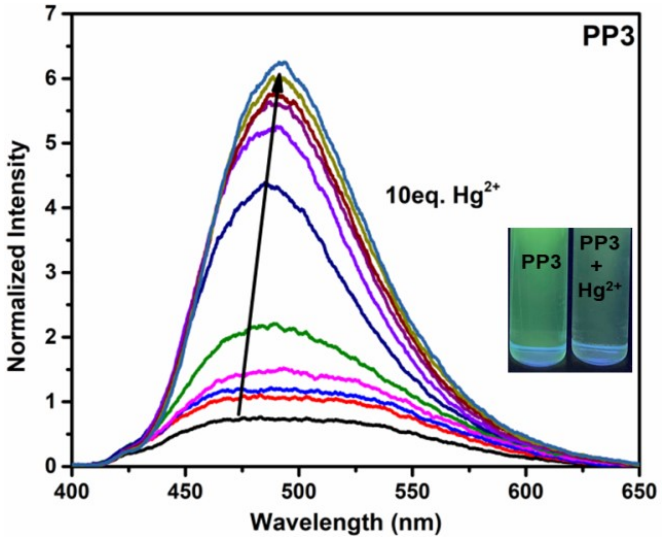
PP3
10eq. Hg2+
Normalized Intensity
Wavelength (nm)
PP3
PP3 + Hg2+

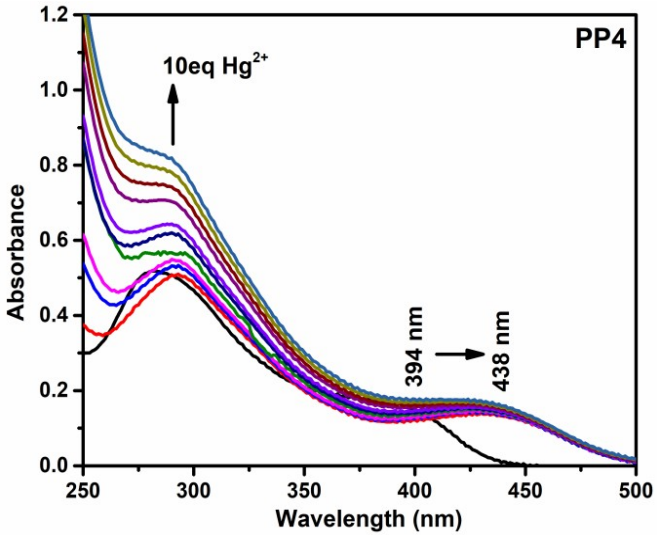
PP4
10eq Hg2+
Absorbance
Wavelength (nm)
394 nm
438 nm

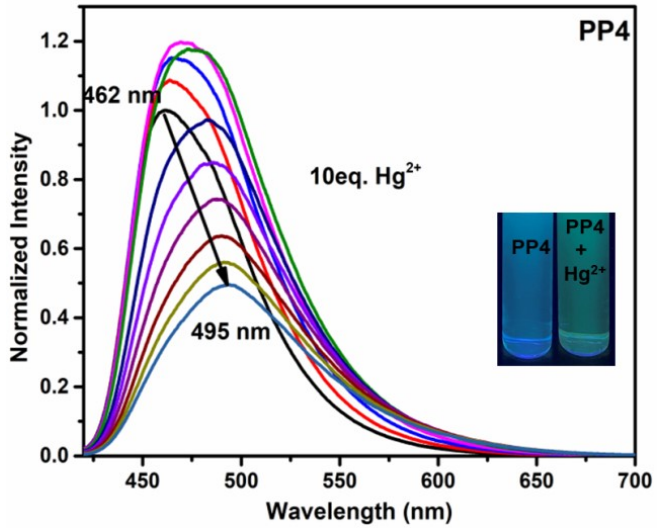
PP4
462 nm
10eq. Hg2+
495 nm
Normalized Intensity
Wavelength (nm)
PP4
PP4 + Hg2+

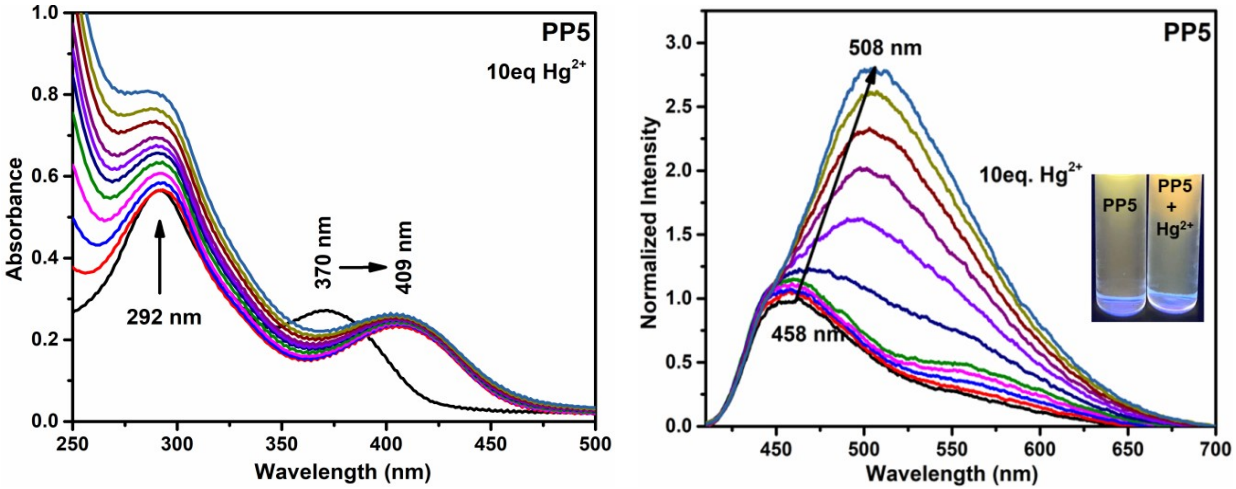

Fig. S26. The emission spectra of **PP2-PP5** as a function of Hg^{2+} equivalents in THF-H_2O mixtues.

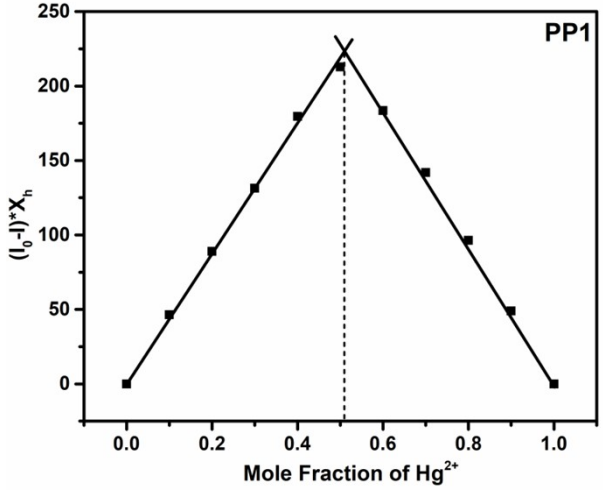

Fig. S27. Job's plot for **PP1** showing 1:1 binding stoichiometry with Hg^{2+}.

Table S4: Limits of detection of **PP1-PP5** for TFA (in $CHCl_3$) and Hg^{2+} ions (in THF-H_2O).

Compounds	D.L. of TFA (μM)	D.L. of Hg^{2+} (nM)
PP1	1.39	11.24
PP2	1.20	18.59
PP3	6.00	26.28
PP4	0.35	2.74
PP5	0.78	9.36

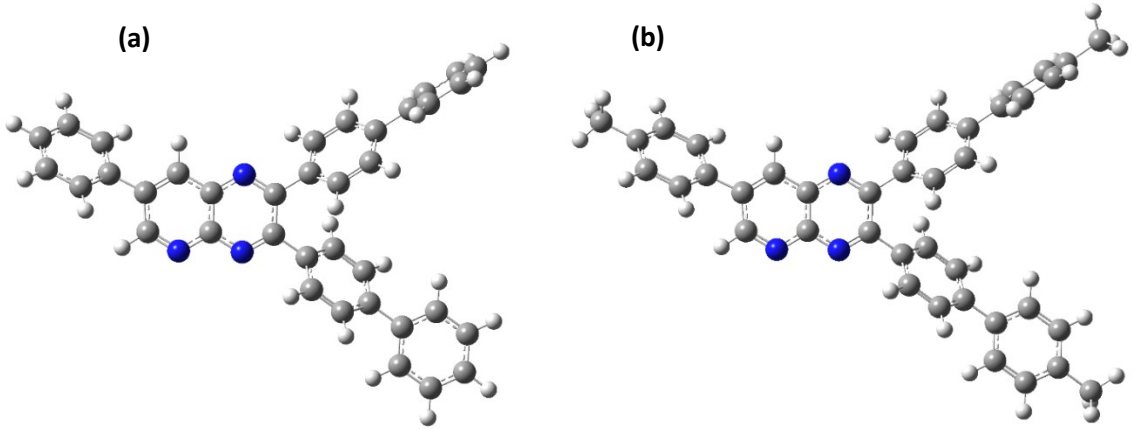

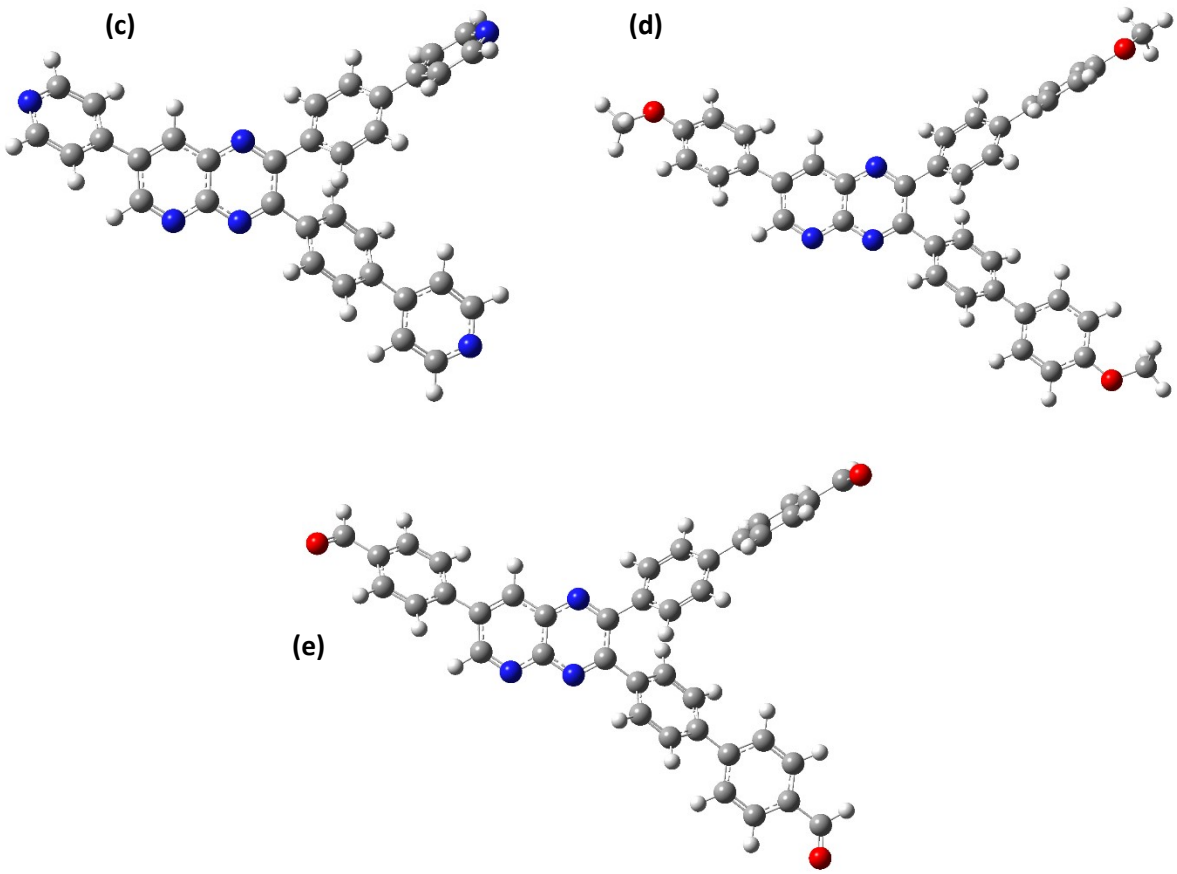

Fig. S28. Optimized structures of (a) PP1, (b) PP2, (c) PP3, (d) PP4, (e) PP5 (Color code: C-grey, N-blue, H-white, O-red).

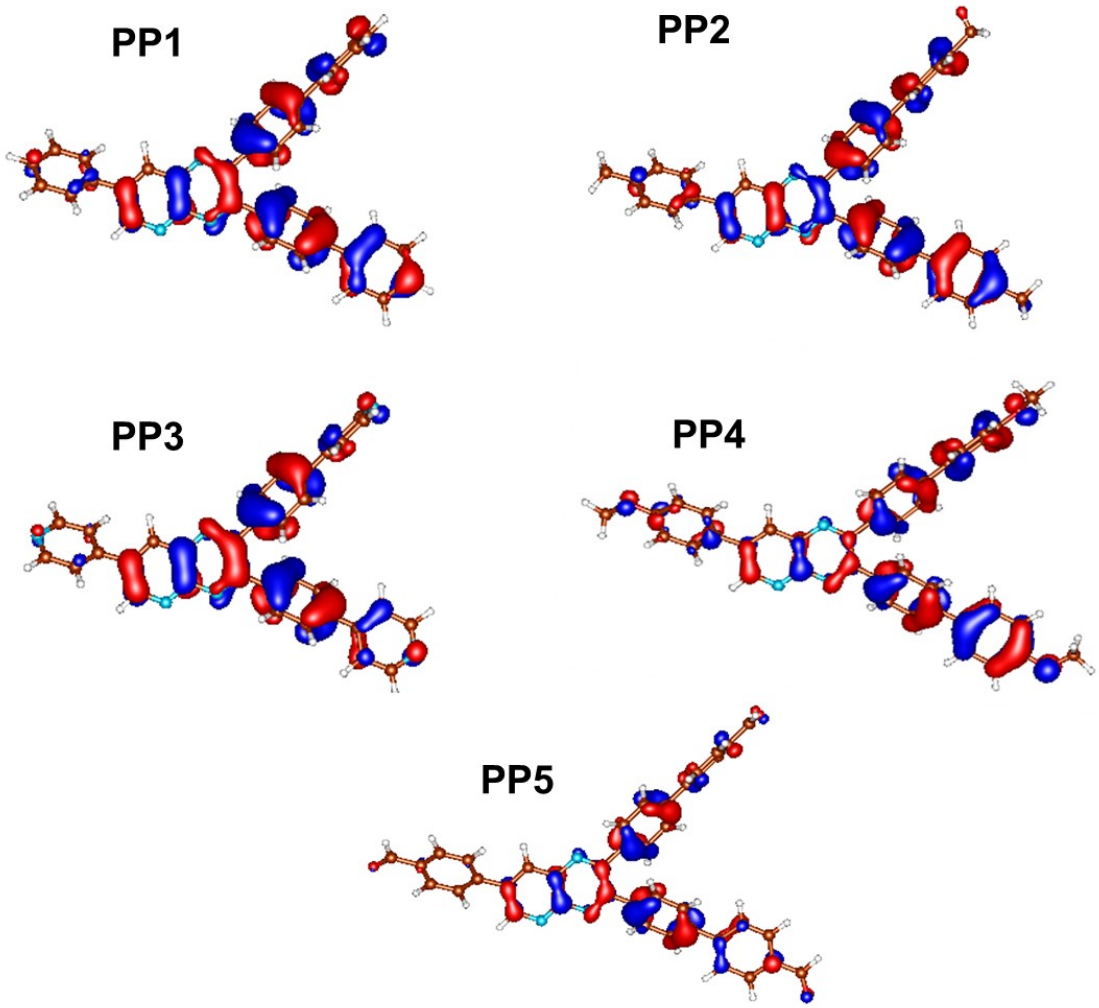

Fig. S29. The HOMO of **PP1**-**PP5**.

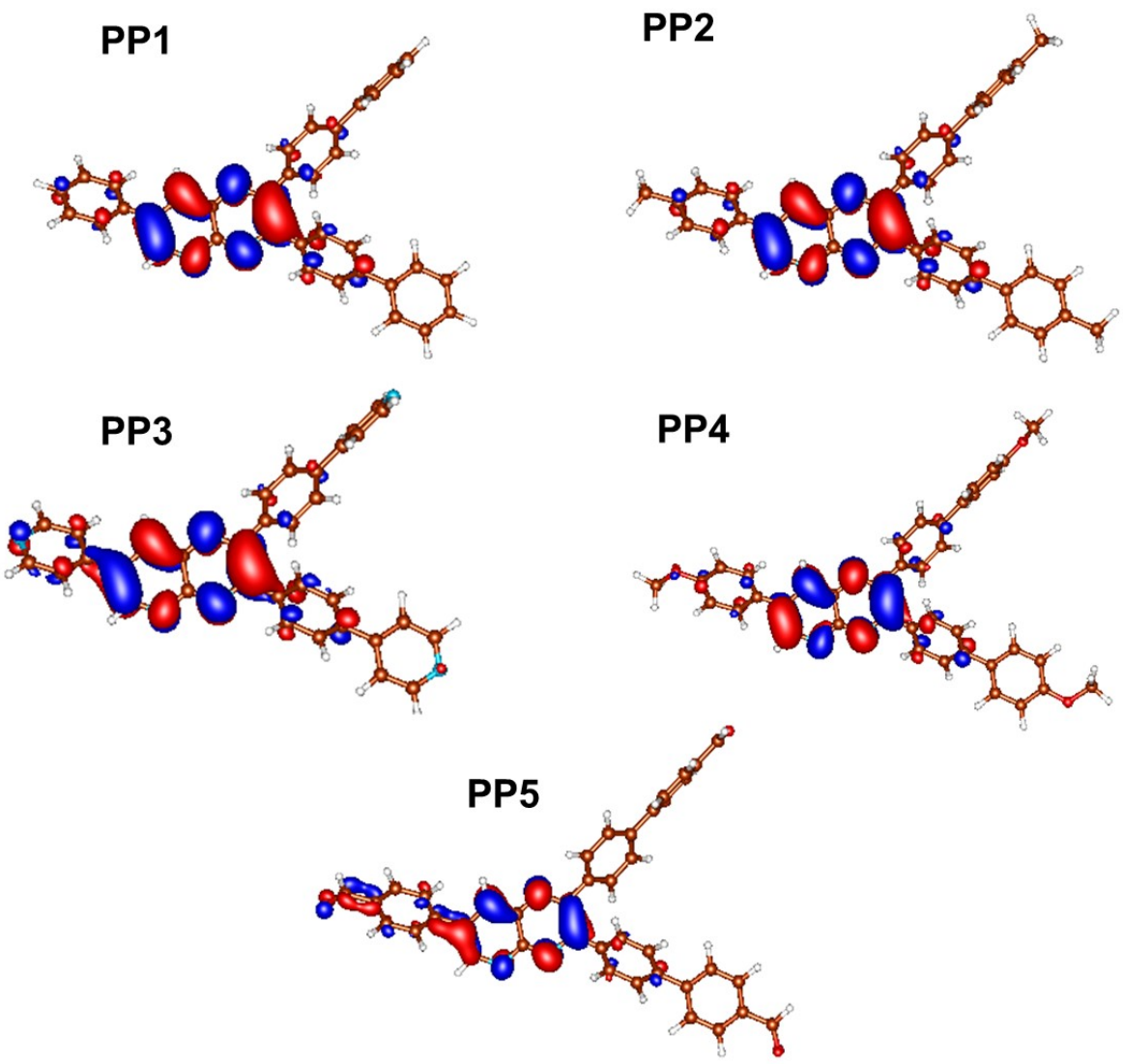

Fig. S30. The LUMO of **PP1**-**PP5**.

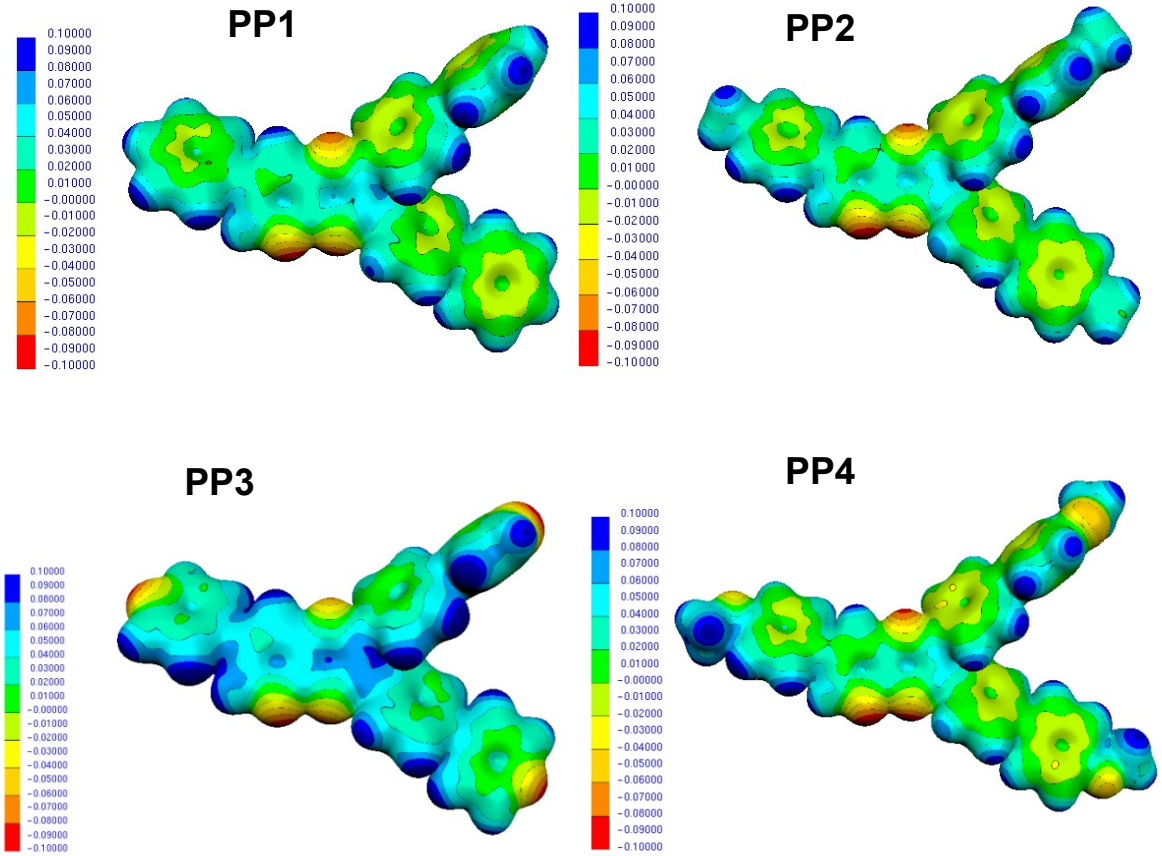
PP1
PP2
PP3
PP4
0.10000
0.09000
0.08000
0.07000
0.06000
0.05000
0.04000
0.03000
0.02000
0.01000
-0.00000
-0.01000
-0.02000
-0.03000
-0.04000
-0.05000
-0.06000
-0.07000
-0.08000
-0.09000
-0.10000

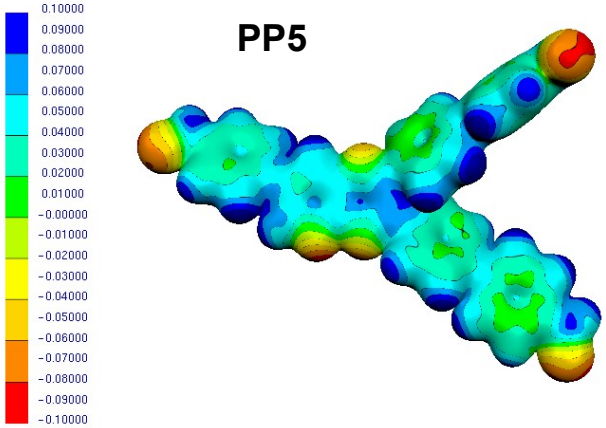

Fig. S31. Electrostatic potential mapped on the electron density surface of **PP1**-**PP5** (iso-value = 0.02 a.u.). Red centers indicate electron-rich centers.

Table S5. Calculated TDDFT absorption and emission wavelengths (nm), oscillator strengths, and major composition in terms of MO contribution for **PP1**-**PP5**.

Compound	λ_{abs} (nm)	Oscillator strengths$_{abs}$	λ_{em} (nm)	Oscillator strengths$_{em}$	Major composition
PP1	390.96	0.8254	467.73	1.1468	HOMO → LUMO (69%)
PP2	400.63	0.8731	478.74	1.2148	HOMO → LUMO (69%)
PP3	376.62	0.6655	410.69	0.9872	HOMO → LUMO (62%)
PP4	419.39	0.8770	499.22	1.2063	HOMO → LUMO (69%)
PP5	392.43	1.1616	482.44	1.7121	HOMO → LUMO (69%)

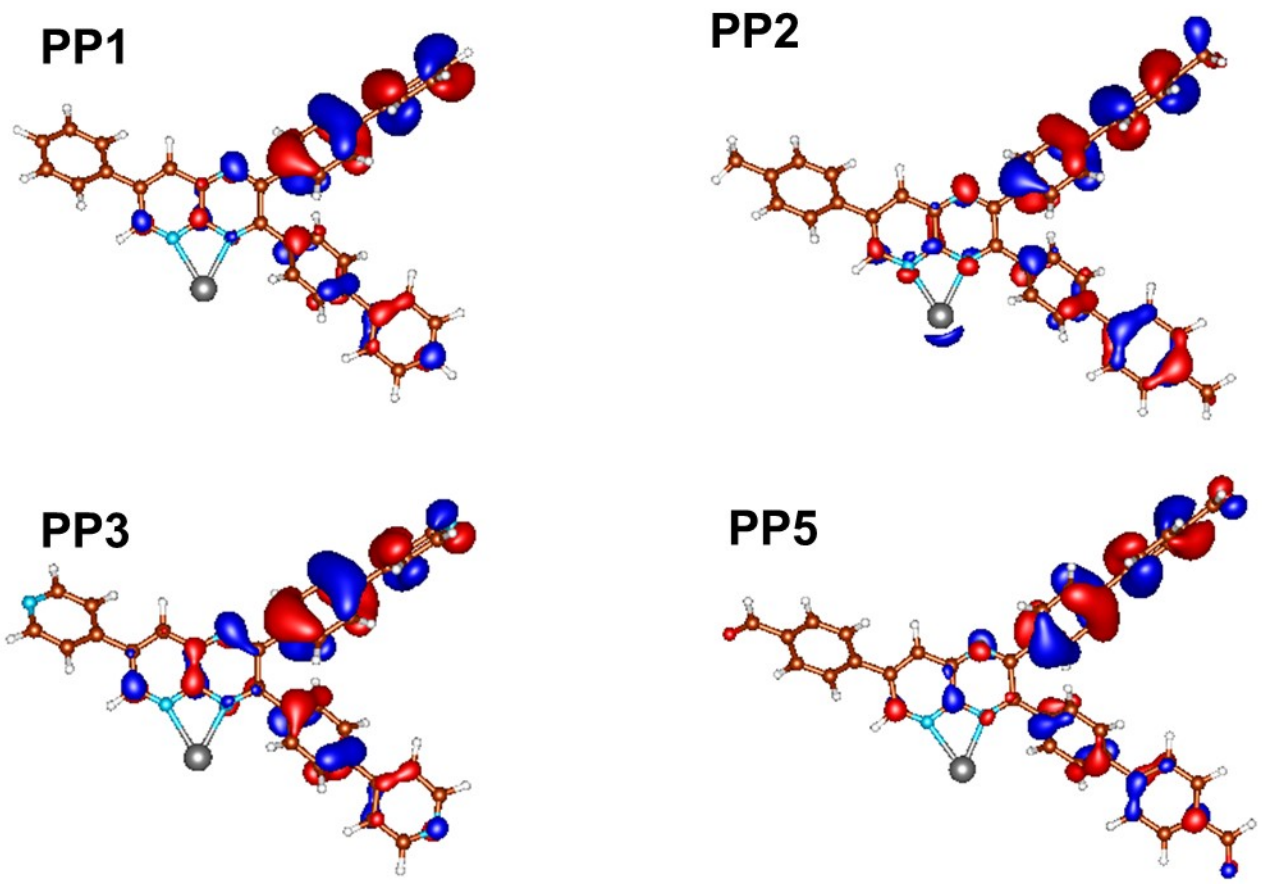

Fig. S32. The HOMO for complexes of Hg^{2+} with **PP1**-**PP3**, **PP5** (iso-value = 0.03 a.u.).

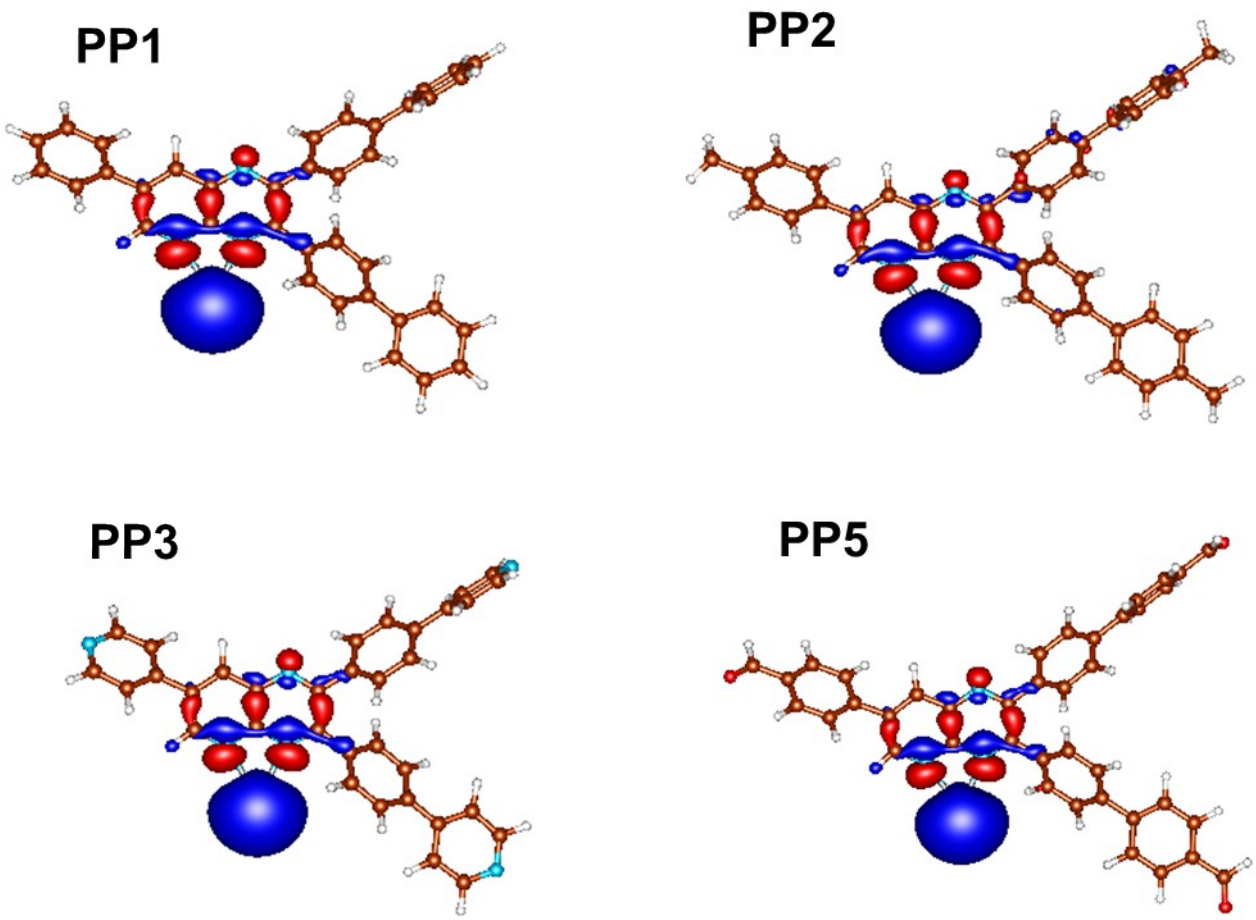

Fig. S33. The LUMO for complexes of Hg^{2+} with **PP1**-**PP3**, **PP5** (iso-value = 0.03 a.u.).

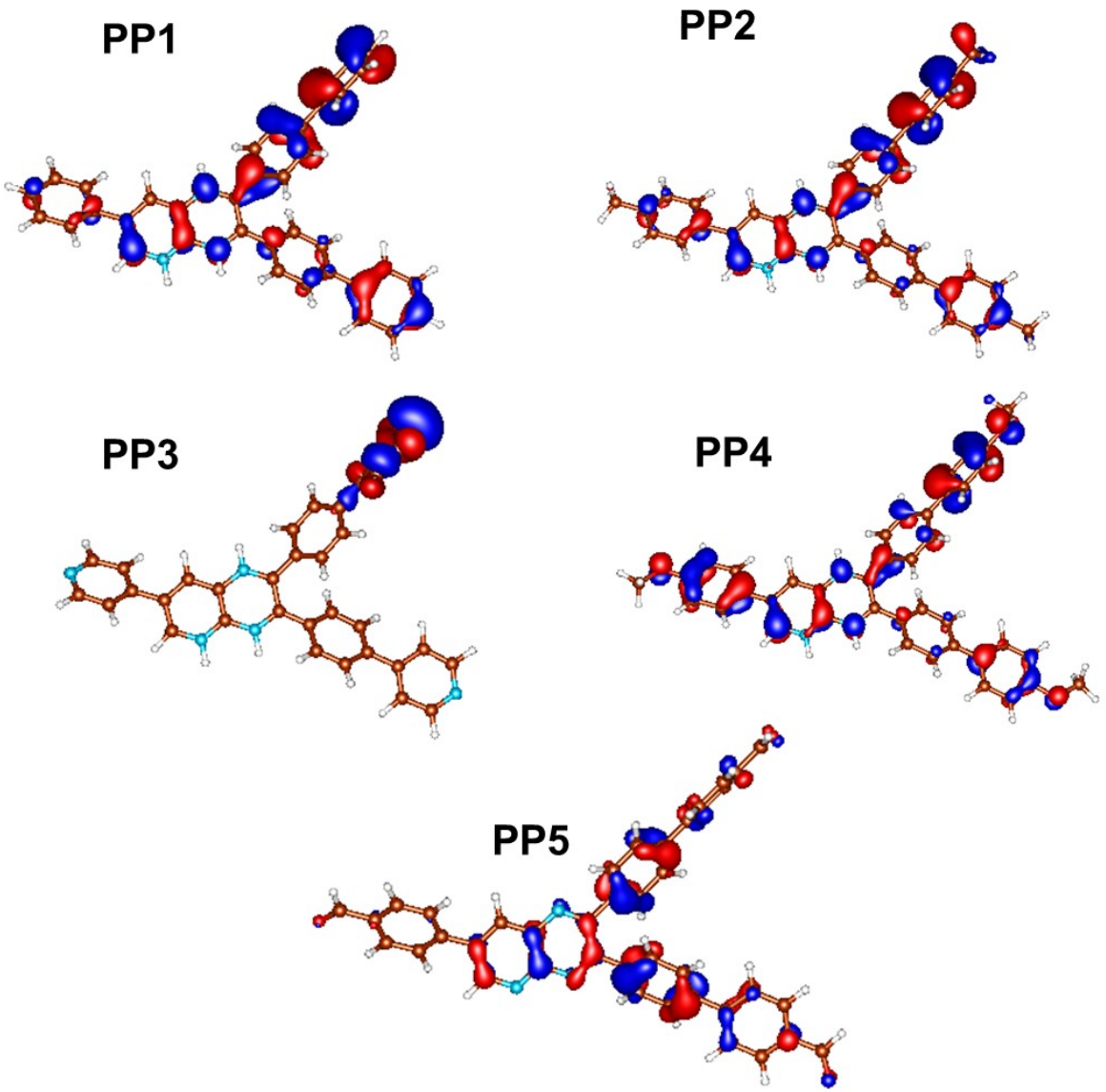

Fig. S34. The HOMO for complexes of TFA with **PP1**-**PP5** (iso-value = 0.03 a.u.).

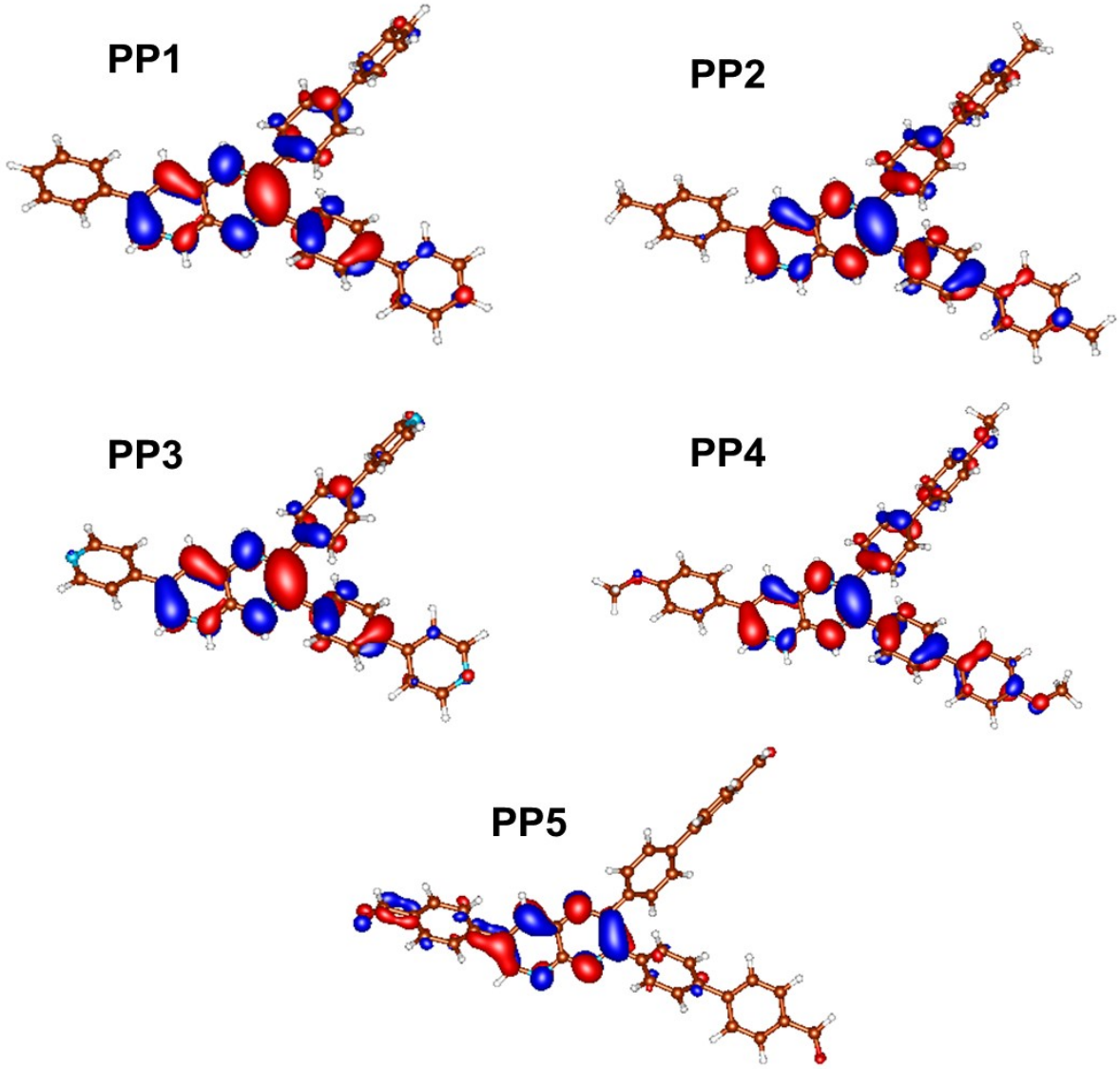

Fig. S35. The LUMO for complexes of TFA with **PP1**-**PP5** (iso-value = 0.03 a.u.).

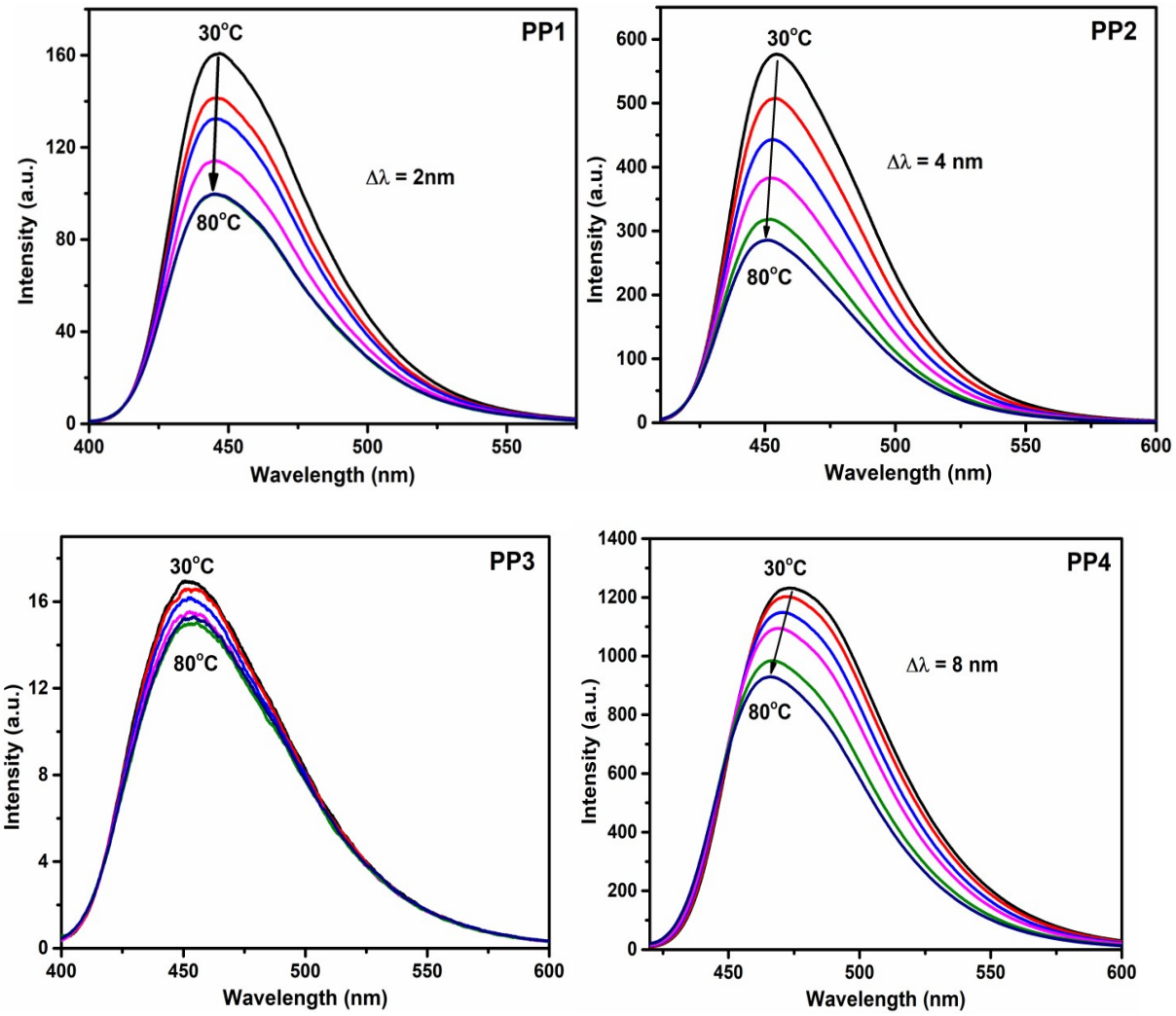
PP1
30°C
80°C
Δλ = 2nm
Intensity (a.u.)
Wavelength (nm)
PP2
30°C
80°C
Δλ = 4 nm
Intensity (a.u.)
Wavelength (nm)
PP3
30°C
80°C
Intensity (a.u.)
Wavelength (nm)
PP4
30°C
80°C
Δλ = 8 nm
Intensity (a.u.)
Wavelength (nm)

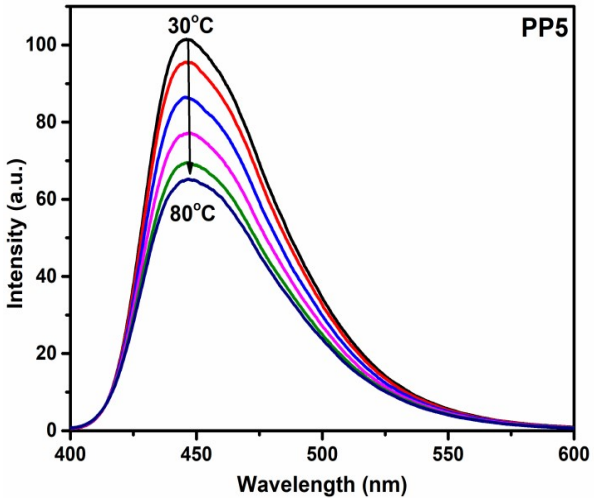

Fig. S36. Temperature dependent changes in the emission spectra of **PP1-PP5** in $CHCl_3$ (1×10^{-5} M).

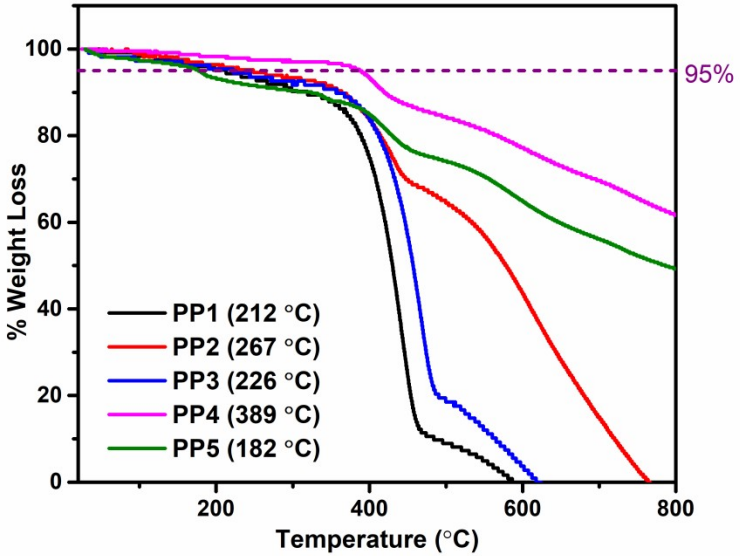

Fig. S37. TGA profiles of **PP1-PP5** representing their decomposition temperatures at 5% weight loss.